Ministère de l'Enseignement Supérieur et de la Recherche scientifique
وزارة التعليم العالي و البحث العلمي

BADJI MOKHTAR-ANNABA UNIVERSITY
UNIVERSITE BADJI MOKHTAR-ANNABA

جامعة باجي مختار- عنابة

Faculté des Sciences de l'Ingéniorat
Département d'Electronique

Année : 2016/2017

THESE

Présentée en vue de l'obtention du diplôme de ***DOCTORAT 3ème cycle***

Compression faible complexité et codage par régions d'intérêt d'images fixes dans les WSNs

(Low complexity image compression and region of interest coding in WSN)

Option

Multimédia et Communications Numériques

Par

MECHOUEK Khaoula

Rapporteur : Mme KADDECHE Nadia MCA Université Badji Mokhtar, Annaba
Co-rapporteur : M. DOGHMANE Noureddine Prof Université Badji Mokhtar Annaba

Devant le Jury

Président :	M. HARKAT Mohamed Faouzi	Prof	Univ ANNABA
Examinateur :	Mme SERIR Amina	Prof	USTHB
Examinateur :	M. BOUKROUCHE Abdelhani	Prof	Univ Guelma
Examinateur :	Mme BOUKARI Karima	MCA	Univ ANNABA

Année Universitaire : 2016/2017

Dedication

This work is dedicated to every student is trying so hard to achieve his goals.

Acknowledgements

I am thankful to ALLAH for giving me strength and ability to complete this research.

I owe deep gratitude to the ones who have contributed greatly in the completion of this thesis.

Foremost, I would like to express my sincere gratitude to Dr Kouadria Nasreddine for his able guidance in this research and for providing me a platform to work on it in this challenging area of research.

I express my sincere gratitude to my supervisor Dr. Kaddeche Nadia, for her support throughout this work.

A particular thanks to my co-supervisor Pr Doghmane Nourddine for his meaningful help and support. And for his insights and attention to details that have been a true inspiration to my research.

I am also very grateful to my thesis committee members, Mrs. SERIR Amina, professor from USTHB University; Mr. BOUKROUCHE Abdelhani, professor from Guelma University; Mrs. BOUKARI Karima MCA from Annaba University and also Mr. HARKAT Mohamed Faouzi professor from Annaba University, for accepting to judge this work of research.

My thanks also go to all those who have helped me to finalize this thesis and to all the teachers who have contributed to my training.

In the last but not the least I am thankful to every member of my big family, and to my parents, my parents in law, my husband, my sisters and my brother, for their blessings and support, which without them it would be impossible to carry out this research.

ملخص

الحد من تعقيد خوارزمية تقنيات ضغط الصور هو تحد كبير في شبكات استشعار الصورة اللاسلكية .العديد من تقنيات ضغط الصور، مثل جيبغ و جيبغ2000، ليست مناسبة للتنفيذ في شبكات استشعار الصورة اللاسلكية بسبب استهلاكها العالي للطاقة الذى يرجع لتعقيدها الحسابي العالي. لحل هذه المشكلة، اقترحنا في هذه الأطروحة بعض خوارزميات ضغط الصورة ذات التعقيد المنخفض استنادا إلى تحويل جيب التمام المنفصل (DCT) وتحويل تشيبشيف المنفصل (DTT). وعلاوة على ذلك، طبقنا عليها نهج تقليم من أجل زيادة الحد من تعقيدها الحسابى ومن ثم استهلاكها الطاقوى. بالإضافة إلى ذلك، اقترحنا ضغط صورة جديد على أساس المصالح باستخدام تحويلDCT. حيث، الفكرة الرئيسية لهذه الطريقة هي ضغط أجزاء معينة من الصورة التي هي ذات أهمية على غرار بقية الصورة. وتبين نتائج المحاكاة أن أساليب الضغط المقترحة تتطلب عددا أقل من العمليات الحسابية، واستهلاك الطاقة والذاكرة. ولها في نفس الوقت كفاءة ضغط تنافسية مقارنة مع أحدث التقنيات لضغط الصورة. و بالتالى تعتبر التقنيات المقترحة خيارات قابلة للتطبيق لضغط الصورة و / أو الاتصالات فى شبكات استشعار الصورة اللاسلكية

الكلمات المفتاحية: شبكات الاستشعار اللاسلكية البصرية, ضغط الصور , حفظ الطاقة , التعقيد الحسابي, تحويل جيبي متقطع, تحويل تشيبتشاف متقطع , تقنية تقليم , ترميز المناطق المهمة

Abstract

Reducing the algorithmic complexity of image compression techniques is a great challenge in wireless image sensor networks (WISNs). Many image compression standards, such as JPEG and JPEG2000, are not suitable for implementation in WISNs because of its high energy consumption due to their high computational complexity. To solve the problem, in this thesis we proposed some low complexity image compression algorithms based on the discrete cosine transform (DCT) and the Discrete Tchebichef transform (DTT). Furthermore, we applied on them the pruned approach in order to more reduce its complexities and thence their energy consumption. Additionally, we proposed a region-of-interest based image compression using the DTT transform. Where, the main idea of this method is to compress certain parts of an image which are of a higher importance in detriment of the rest of the image. Simulation results show that the proposed compression methods require a reduced number of arithmetic operations, energy consumption and memory. And they have at the same time competitive compression efficiency compared with state-of-the-art image compression techniques which make them viable options for image compression and/or communication over WISNs.

Keywords: WISNs, image compression, Arithmetic complexity, energy consumption, DCT, DTT, pruned approach, Region-of-interest coding.

Résumé

Réduire la complexité algorithmique des techniques de compression d'image est un grand défi dans les réseaux de capteurs d'image sans fil (RCISFs). De nombreuses normes de compression d'image, telles que JPEG et JPEG2000, ne sont pas adaptées à une implémentation dans les RCISFs en raison de leur forte consommation énergétique à cause de leur complexité élevée. Pour résoudre le problème, dans cette thèse, nous avons proposé des algorithmes de compression d'image de faible complexité basés sur la transformée en cosinus discrète (TCD) et la transformée de Tchebichef discrète (TTD). En outre, nous avons appliqué l'approche zonale afin de réduire davantage ses complexités et donc leur consommation d'énergie. De plus, nous avons proposé une technique de compression d'image des régions d'intérêt basée sur la TTD. Où, l'idée principale de cette méthode est de compresser certaines parties d'une image qui sont importantes au détriment du reste de l'image. Les résultats de simulation montrent que les méthodes de compression proposées nécessitent un nombre réduit d'opérations arithmétiques, de consommation d'énergie et de mémoire. Et ils ont en même temps une efficacité de compression comparable aux techniques de compression d'image bien connues dans la littérature. Ces performances les rendent viables pour la compression et / ou la communication d'images sur les RCISFs.

Mots clés: RCISFs, compression d'image, complexité arithmétique, consommation d'énergie, TCD, TTD, Codage par région d'intérêts.

List of Abbreviations

1-D one-dimensional

2-D two-dimensional

AC Alternative Components

ADC Analog to Digital Converter

ASIC Application-Specific Integrated Circuit

BDCT Binary Discrete Cosine Transform

Bps bit per pixels

CCD Charge Coupled Device

DCT 1D Discrete Cosine Transform one dimensional

DCT 2D Discrete Cosine Transform two dimensional

CMOS Complementary Metal Oxide Semiconductor

DA Distributed Arithmetic

DC Direct Component

DFT Discrete Fourier Transform

DTT Discrete Tchebichef Transform

DWT Discrete Wavelet Transform

EBCOT Embedded Block Coding with Optimised Truncation

EZW Embedded Zerotree Wavelet

FDCT Forward Discrete Cosine Transform

FOV Field Of View

FPGA Field Programmable Gate Array

GPS Global Positioning system

HH High High

HL High Low

HVS Human Visual System

JPEG Joint Photographic Experts Group

JPEG2000 Joint Photographic Experts Group 2000

Kbps Kilo bit per pixels

KLT Karhunen-Loeve Transform

LH Low High

LL Low Low

LZW Lempel-Ziv-Welch

MCU Micro-Controller Unit

MRDCT Modified Rounded Discrete Cosine Transform

mW MilliWatt

SAD Sum of absolute difference

SSIM Structural SIMilarity index metric

MSE Mean Square Error

P-BDCT Pruned Binary

PDA Personal Digital Assistant

P-DCT Pruned Discrete Cosine Transform

P-DTT Pruned Discrete Tchebichef Transform

PSNR Peak Signal to Noise Ratio

QCIF Quart Common Intermediate Format

QoS Quality of Service

RDCT Rounded Discrete Cosine Transform

RF Radio Frequency

RLC Run Length Coding

ROI Region Of Interest

SDCT Signed Discrete Cosine Transform

SFG Signal Flow Graph

SPIHT Set Partitioning In Hierarchical Trees

VLC Variable-length code

WCH Wireless Cluster Head

WHT Walsh Hadamard Transform

WISN Wireless Image Sensor Network

WMN Wireless Multimedia Node

WMSN Wireless Multimedia Sensor Network

WSN Wireless Sensor Network

List of Figures

List of Tables

List of publications

Journal publications:

- **Mechouek**, **K**., Kouadria, N., Doghmane, N., & Kaddeche, N. (2016*)." Low Complexity DCT Approximation for Image Compression in Wireless Image Sensor Networks".* Journal of Circuits, Systems and Computers (**World scientific**), 25(08), 1650088. ***IF=0.35***

- Kouadria, N., **Mechouek, K**., Messadeg, D., & Doghmane, N. (2017*)." Pruned discrete Tchebichef transform for image coding in wireless multimedia sensor networks". AEU*-International Journal of Electronics and Communications (**Elsevier**), 74, 123-127. ***IF=1,15***

Conference publications

- Kouadria, N., **Mechouek, K**., & Doghmane, N. *"Energy efficient 8 by 8 DCT approximation for image compression in wireless image sensor networks",* ICESTI'16, Annaba 2016

- **Mechouek, K**., Kouadria, N., Doghmane, N., & Kaddeche, N., *"Pruned DTT transform for image coding",* ICATS 2015, Annaba

- **Mechouek, K**., Kouadria, N., S, Harize., & Doghmane, N. ,"*Extension of the hybrid transforms DCT-DWT to color images"* CESTI'14, Annaba Novembre 2014

- Kouadria, N., Doghmane, N., & **Mechouek, K**. ,"*New Approach of Zonal Integer DCT for Image Compression in Wireless Image Sensor Networks",* CESTI'14, Annaba, Novembre 2014

Contents

Chapter 3: *Proposed low complexity image compressions*

General introduction

Introduction

Wireless sensor networks (WSNs) are one of the promising technologies for the future, where a close interaction with the physical world is essential. Which make us living in a world of connected things, objects and devices. These emerging tiny devices can detect and evaluate different type of data depends of course on the desired applications, and send back the data automatically to us.

WSNs offer a lot of advantages over the classic networks solutions such as low cost, scalability, reliability, flexibility and also the ease of deployment. All these factors together open the door to use them in different applications like in military, environment, healthcare, and security. In military, sensor nodes can be used to detect, locate, or track enemy movements. In case of natural disasters, sensor nodes can sense and detect the environment to forecast disasters in advance. In healthcare, sensor nodes can help in monitoring a patient's health. In security, sensors can offer vigilant surveillance and increase alertness to potential terrorist attacks.

However, the main obstacle over the development of these networks is the limited power supply and the high energy consumption. Therefore many techniques of energy efficiency have been used in wireless sensor networks in order to minimize the energy consumption in every single sensor nodes which leads at maximizing the lifetime of the whole network.

Wireless multimedia sensor networks (WMSNs) are a specific case, which deals with a large amount of data such as videos, images and even scalar data. In this case, an additional effort is really necessary in order to be able to reduce the energy consumption on these nodes like doing a low complexity image and video compression.

Real time processing and transmission using these devices requires image compression algorithms that can compress efficiently with reduced complexity. Due to limited resources, it is not always possible to implement the best algorithms inside these devices. In uncompressed form, both raw and image data occupy a huge amount of space. However, both raw and image data have a significant amount of statistical and visual redundancy. Consequently, the used storage space can be efficiently reduced by compression. In this thesis, a novel low complexity and embedded image compression algorithms are developed especially suitable for low bit rate image compression using these tiny devices.

However, in some cases we need some regions on the compressed image to be clear in order to be able to identify and recognize some important details such as: faces, moving

objects…etc. So, the need of region of interest (ROI) coding is necessary in WSNs. The main idea of this coding is to compress and transmit only certain parts of an image which are of a higher importance to the end applications user (i.e. tracking, identification, recognition …etc) in detriment of the rest of the image.

Thesis outlines

This thesis is organized as follows:

In chapter 1, we will give a survey of wireless networks including wireless multimedia sensor networks and we will focus our study on energy conservation problems. Where, we describe the hardware design of a sensor node and we present the key features that influence its design, and we describe in detail the communication process in the network. Also, we will focus on energy problems and we will present a detailed explanation on power dissipation and the reasons of energy waste in wireless sensor networks. We end the chapter with the state-of-the-art solutions to these problems by the classification of energy efficiency techniques.

In chapter 2, we will focus on the available image compression algorithms and techniques under the constraints of WMSNs and explore their theoretical limits on achievable compression. We will also describe some standards of image compression like JPEG, JPEG2000 and SPIHT and their possible integration to WMSNs

In chapter 3, we will propose new DCTs approximations to more reduce the arithmetic complexity and also to maintain a good image quality. Thus, we will have a good trade-off quality /complexity, which is suitable for resource constrained low-power sensors nodes. Also we will prove that the discrete Tchebichef transform (DTT) is a useful tool in image and video compression. Thence we will propose a pruned discrete tchebichef transform (P-DTT) that exhibits low computational complexity and good image compression performance in terms of peak signal to noise ratio (PSNR) and structural similarity index (SSIM).

Finally, chapter 4 will concern the region of interest coding. Where, we will propose a ROI-based image compression. We presents the principles of this proposed method and evaluate it in terms of quality of received images, transmission energy, processing energy and the amount of transmitted data. We will give an extensive comparison to others state-of-the-art methods and we will show the efficiency of the proposed compression techniques.

Chapter 1

Introduction to wireless sensor networks

1.1. Introduction:

Wireless sensor network (WSN) has attracted much attention in recent years, and it has emerged as one of the most promising technologies for the future. They are used in many applications, where a close interaction with the physical world is essential. The simple deployment and the distributed sensing properties provided by a wireless communication system make WSNs an important component of our daily lives.

WSN technology offers numerous advantages over the classical existed networks, where the most important fact is the ease of deployment that allows their use in a wide range of diverse applications [1]. With advancements in this field of research and sensors getting smarter, smaller, and cheaper, a huge number of wireless sensors are being deployed in numerous applications. Some of the potential application domains are military, environment [2-4], healthcare [5-7], and security. In military [8-10], sensor nodes can be used to detect, locate, or track enemy movements everywhere and at any time. In case of natural disasters, sensor nodes can sense and detect the environment to predict disasters in advance. In healthcare, sensor nodes can help in monitoring the health of patients and also to make a remote coordination between doctors and their patients. In security, sensors can offer vigilant surveillance and increase the caution to potential terrorist attacks.

A sensor network is composed of a large number of tiny devices called sensor nodes, where each node is connected to one or several sensors. Each sensor network node has typically several parts: a radio transceiver with an internal antenna or connection to an external antenna, a microcontroller, an electronic circuit for interfacing with the sensors and an energy source, usually a battery or an embedded form of energy harvesting.

Sensor nodes are densely deployed either inside the phenomenon or very close to it and their position do not need to be engineered or pre-determined, this allows random deployment in inaccessible areas. On the other hand, this also means that sensor network protocols and algorithms must possess self-organizing capabilities.

One of the most important constraints on sensor nodes is the low power consumption requirement. Sensor nodes have limited power sources. Therefore, while traditional networks aim to achieve high quality of service (QoS) provisions, sensor network protocols must focus primarily on power conservation. They must have inbuilt trade-off mechanisms that give the end user the option of prolonging network lifetime at the cost of lower throughput or higher transmission delay.

In this chapter, we will present a survey of wireless networks and focus our study on energy conservation problems. In section 1.2, we will give an overview on wireless sensor networks describing the hardware design of a sensor node and present the factors that influence on wireless sensor network functioning. Section 1.3 details the communication process for sending and receiving a specific data in the wireless sensor network. Section 1.4 focuses on energy problems and present a detailed explanation on power dissipation and the reasons of energy waste in wireless sensor networks. We will also try to give a solution to these problems by the classification of energy efficiency techniques. Finally, a general overview on wireless multimedia sensor networks and theirs characteristics is given in section 1.5.

1.2. Wireless sensor networks characteristics

The design of WSNs requires a huge knowledge of a wide variety of research fields including wireless communication, networking, embedded systems, digital signal processing, and software engineering. This is motivated by the close coupling between several hardware entities of wireless sensor devices as well as the distributed operation of a network of these devices.

1.2.1. Internal structure of a sensor node:

Figure 1.1 illustrates the most common scheme of sensor node design. Also the main blocks of each sensor node are represented. Generally, it is contains on four basic components as shown in Fig. 1: a sensing unit, a processing unit, a transceiver unit and a power supply unit. They may also have application dependent additional components [11] such as a location finding system, a power generator and a mobilizer.

Sensing unit: it may generally include several sensor units and each sensor unit is responsible for gathering information of certain type such as: temperature, humidity, or light… etc. they usually composed of two subunits: sensors and analog to digital converters (ADCs). The analog signals produced by the sensors based on the observed phenomenon are converted to digital signals by the ADC, and then fed into the processing unit.

***Processing unit*:** which is generally associated with a small storage unit, the processing unit manages the procedures that enable the sensor node to perform sensing operations, run associated algorithms, and collaborate with the other nodes through wireless communication [12]. *Microcontrollers* carry out the function of controlling all the components, and also process data received from sensing element of this sensor node, as well as data received from other sensor nodes. Microcontrollers are widely used as control elements in a sensor node, by

the reason of their low cost, low energy consumption, small size. And also, the ability of finding easily additional modules with various digital and even wireless interfaces, and also with the necessary performance.

***Transceiver unit*:** communication between any two wireless nodes is performed by the transceiver units. A transceiver unit implements the necessary procedures to convert bits to be transmitted into radio frequency (RF) waves and recover them at the other end. Essentially, the WSN is connected to the network through this unit.

Power supply unit: One of the most important components of a sensor node is the power supply unit.

Usually, battery power is used, but also other energy sources are also possible. Each component in the wireless sensor node is powered through this unit and the limited capacity requires energy-efficient operation for the tasks performed by each component [11].

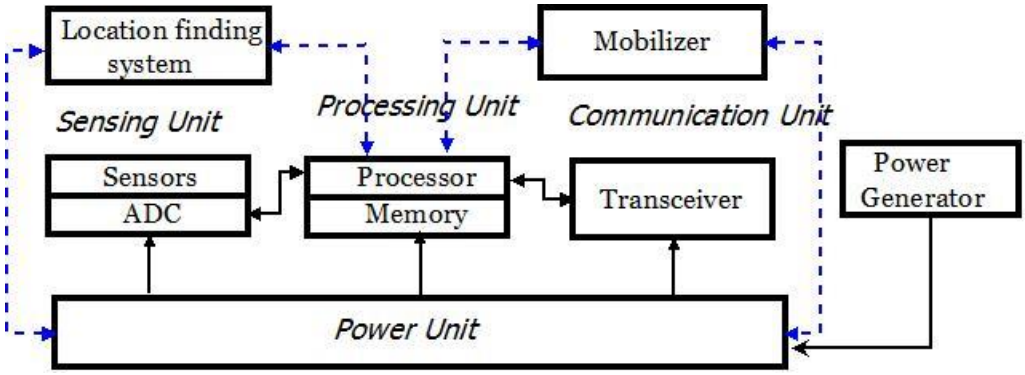

Figure1.1. *Hardware architecture of a sensor node*

***Location finding system*:** Most of the sensor network applications, sensing tasks, and routing techniques need knowledge of the physical location of a node. This module system may consist of a GPS module for a high-end sensor node or may be a software module that implements the localization algorithms providing location information through distributed calculations.

Mobilizer: A mobilizer may sometimes be needed to move sensor nodes when it is necessary to carry out the assigned tasks. Mobility support requires extensive energy resources and should be provided efficiently.

Power generator: While battery power is mostly used in sensor nodes, an additional power generator can be used for applications where longer network lifetime is essential. For outdoor applications, solar cells can be used to generate power. Similarly, energy harvesting techniques for thermal, kinetic, and vibration energy can also be used [13].

1.2.2 Key features influencing sensor network design:

Before designing any sensor node, we must take into consideration the main features and factors that affect directly the capabilities of the whole WSN. The most important of these factors are platform flexibility and scalability; production size and costs; sensor network topology; reliability; power consumption, transceiver Performances and information security. These factors [11] have been addressed by many researchers in a wide range of areas concerning the design and deployment of WSNs. Moreover, the integration of solutions for these factors is still a major challenge because of the interdisciplinary nature of this area of research.

Platform flexibility and scalability: The number of sensor nodes deployed to study a phenomenon may be in the order of hundreds or thousands. Therefore, the networking protocols developed for these networks should be able to handle these large numbers of nodes. The density can range from a few to hundreds of sensor nodes in a region, which can be less than 10m in diameter. The node density depends on the application for which the sensor nodes are deployed. Moreover, the majority of real applications require flexibility and adaptability of the WSN platform. However, each sensor node platform must have the ability to be adjusted to meet the requirements of a specific application.

Production size and costs: Miniaturization, price reduction and the diversity of applications are the keys that lead to the widespread use of WSNs. And since the sensor networks consist of a large number of sensor nodes, the cost of a single node is very important to justify the overall cost of the networks. If the cost of the network is more expensive than deploying traditional sensors, then the sensor network cost cannot be justified. As a result, the cost of each sensor node has to be kept low. Note that a sensor node also has some additional units such as sensing and processing units. In addition, it may be equipped with a location finding system, cameras, mobilizer, or power generator depending on the applications of the sensor networks. As a result, the cost of a sensor node is a very challenging issue and it is proportional to a given amount of functionalities.

Energy consumption: The main concern for operation of WSNs is the energy consumption. For most applications, the sensor nodes are deployed in hard to access areas which make it not feasible to replace batteries of the sensor nodes. Thus, a WSN is required to operate for a long time over months or even years in order to reduce maintenance intervention and gain in time and cost.

Reliability: Reliability in a WSN is the ability of the network to maintain its functionality regardless of the failure of nodes because some sensor may fail or be blocked because of lack of power, physical damage, or environmental interference [14-16]. This should not affect the overall task of sensor network.

Transceiver Performance: One of the key sensor node characteristics is transceiver performance. The main parameters of transceiver performance which affect the sensor node characteristics are maximum data transfer rate, frequency range, modulation method, receiver sensitivity and transmitter power.

In the transceiver parameter between two sensor nodes in WSN has a direct relation between the power of sensor node transmitter and the impact of the interference in the quality of transmitted signal, so the maximum distance allowed between two consecutives sensor nodes specifies the minimum number of sensor nodes necessary for covering the given space by WSN.

Sensor node receiver *sensitivity* represents the ability to receive weak signals. However, increasing the power and sensitivity of sensor node transmitter and receiver leads to higher energy consumption and cost of the sensor nodes. Thus, the benefit in increasing the range of sensor node is not so great. That is why the most common characteristics of transceivers measure up with ones mW of power, which is acceptable in terms of energy consumption and provides reliable wireless connection between sensor nodes at the distance of about 10 meters.

Frequency range of transceiver affects the maximum possible rate of data exchange and the maximum possible distance between the sensor nodes and also the size of the transceiver antenna. Concerning the rate transfer, it is clear the higher is speed of transmission, the less time is necessary for transmitting the same data; hence, transceiver will be switched on for less time. But high speed of transmitting also requires more computing power and energy for this computing, which is not always acceptable in wireless sensor networks constraints.

Sensor network topology: For the raison of its high density in the observed area, sensor nodes must be able to adapt their functionalities in order to maintain the desired topology.

Information security: In wireless sensor network, there are some applications like in applications used in military where the information security is a very important task. In order to meet the security requirements, sensor nodes must be capable of performing complex encrypting and authentication algorithms.

In fact, radio communication channels and the internal memory of a sensor node can be easily tapped and become available for intruders. For communication channel, the only way to avoid it is encrypting of all data transmitted in the WSN by adding an encryption module to the sensor node device and the level of sophistication depends on the required application. But in any case, encryption requires additional expenditure of energy, and it has negative impact on WSN lifetime.

1.3. Sensor networks communication architecture

1.3.1 Overview of the network architecture:

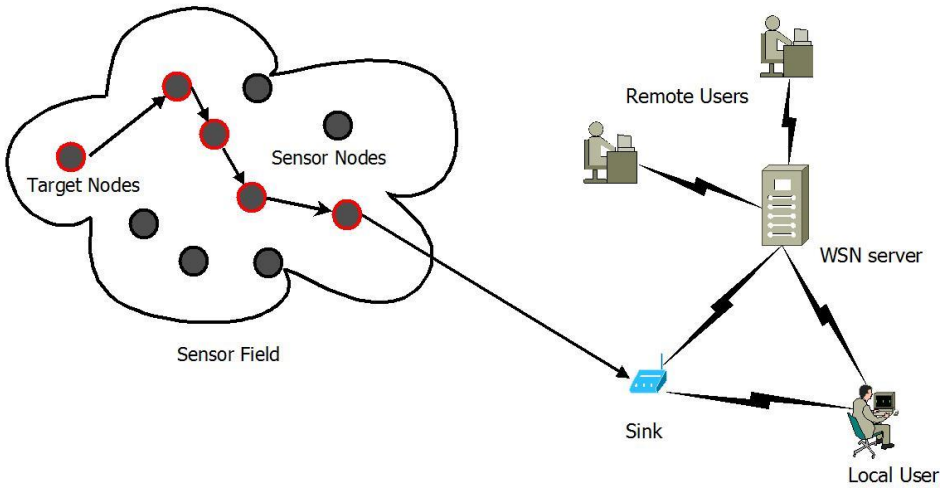

Figure.1.2. *Wireless Sensor Networks (WSNs) structure.*

Sensors networks are a type of wireless networks similar to ad-hoc mobile networks [17]. WSNs are spatially distributed systems which consist of high number of sensor nodes, it could be about dozens, hundreds or even thousands sensor of these devices. They are interconnected with each other through a wireless connection channel to form a single network.

Usually sensor node is an autonomous device. Each sensor node in a WSN measures some physical conditions, such as temperature, humidity, pressure, vibration, and converts them into digital data. After that, it processes the data and stores it in order to transmit them back to the sink and then to the user.

A network sink is a kind of a sensor node which aggregates useful data from other sensor nodes. As a rule, network sink has a stationary power source and is connected to a *server* which is processing data received from WSN. Such connection is implemented directly, if

server and WSN are placed on the same object. The interconnection of the sink with an infrastructure network for example internet with a satellite linkage, allows the remote interconnection of the sensor nodes with the user as it is shown in figure1.2. In this case, the sink plays the role of a gate with the external world.

In some cases sensor nodes get in sort of difficult situations where establishing connection with other sensor nodes is not easy. So, successful WSN deployment depends on both the hardware characteristic and the network self-organization protocols which are used.

1.3.2 Sensor networks communication

In WSNs communication is implemented through wireless transmission channel using low power transceivers of sensor nodes. Communication range of such transceivers is set up in the first place for reasons of energy efficiency. So, the sensor node transceiver has limited energy content so a limited range for transmission, this fact makes it impossible for the most spatially remote sensor nodes to transmit their data directly to the sink. So, in WSN every sensor node transmits its data only to a few of its neighbors which, in their turn, they retransmit those data to their nearest sensor nodes and so on. As a result, after a lot of retransmissions the data finally reach the network sink.

However, the sensor node may turn off its receiver after receiving a message from one of its neighbors in order to avoid getting duplicated messages. Also, when the power level of the sensor node is low, the sensor node broadcasts to its neighbors that it is low in power and cannot participate in routing messages. So, the remaining power will be reserved for sensing only.

The microcontroller in each sensor node is the one responsible for collecting data and connecting with other sensor nodes. Microcontroller firmware has a set of algorithms to control the transceiver and the sensing element. These algorithms make it possible to provide an automatic and autonomous sensor node functioning. So, the microcontroller detects and registers the movement of sensor nodes and keeps track of who are their neighbor sensor nodes. By knowing who the neighbor sensor nodes are, the sensor nodes can balance their power and task usage.

WSN has a self-organization feature, in case there is a connection problem with some sensor nodes, it does not make the whole system fail, but the sensor nodes adapt themselves automatically which simplify their installation and maintenance. This fact makes WSN more

reliable because network reconstruction can be done in real-time mode, and it allows the WSN to quickly react to the environment changes or sensor nodes failures. In addition, self-organization algorithms can provide optimization of energy consumption for data transmission. From the whole sensor network standpoint, the collaboration between the sensor nodes in each WSN is so efficient, so the lifetime of the sensor networks can be prolonged.

Data collected by all the sensor nodes are usually transmitted to the server which provides the final processing of all the information collected by the sensor nodes. In general, a WSN includes one or a few sinks and gates which are collecting data from all the sensor nodes and transmitting these data for further processing. At the same time, gate forwards the data from the WSN to other networks. In this way communication between WSNs and other external networks, like the Internet, is being provided.

1.4. Wireless sensor networks and energy problems

1.4.1 Power dissipation in a wireless sensor node :

In order to find an efficient solution for energy conservation, we must identify power bottlenecks in the system of a wireless sensor node. In this section we analyze a sensor node from a power consumption perspective and discuss which units can significantly impact the system energy consumption.

Microcontroller Unit: The power-performance characteristics of MCUs have been studied extensively, and several techniques have been proposed to estimate the power consumption of these embedded processors [18], [19]. While the choice of MCU is dedicated by the required performance levels, it can also significantly impact the node power dissipation characteristics. A microcontroller can operate in the energy-saving mode (or *active, idle, and sleep* modes). It can shut down most of its inner blocks and then turn them on again. Power consumption can be reduced up to 1000 times in this mode. For power management purposes, each mode is characterized by a different amount of power consumption. According to the example in [20], the Strong-ARM consumes 50 mW of power in the *idle* mode which means the sensor node is listening and waiting to receive the data, and just 0.16mW in the Sleep mode. However, transitioning between operating modes involves a power and latency, overhead. So, the power consumption levels of the various modes, the transition costs, and the amount of time spent by the MCU in each mode all have a significant energy consumption which influence on the battery lifetime of the sensor node.

Radio: Generally, Transceivers which provides access to the radio channel are with a low-rate and short-range. According to [21], some transceivers used in sensor nodes operate at a transfer rate to 250 kbps and distances about 10 m. However, several factors affect the power consumption characteristics of a radio, including the type of modulation, data rate; transmit power, and the operational duty cycle. In general, radios can operate in four distinct modes of operation: *transmit*, *receive*, *idle*, and *sleep*. In the case of *idle* mode the power consumption is significantly high, almost equal to the power consumed in the *receive* mode [22]. Thus, when the sensor node is not transmitting or receiving any data, it is important to completely shut down the radio rather than transitioning to *idle* mode. Another relevant factor is that as mode changes, the transitory activity causes a significant amount of power dissipation in the radio electronics. According to [20], when the radio switches from sleep mode to transmit mode to send a packet, a significant amount of power is consumed for starting up the transmitter itself [23].

Sensors: Sensing is the task for a sensor device which is created for, and each sensor node in WSN measures some physical conditions and it translates the physical phenomena to electrical signals. There are several sources of power consumption in a sensor, including: signal sampling and conversion of physical signals to electrical ones; signal conditioning, and analog-to-digital conversion. In general, passive sensors such as temperature, seismic, etc., consume negligible power relative to other components of sensor node. However, active sensors such as sonar rangers, array sensors such as imagers, and narrow field-of-view sensors that require repositioning such as cameras with pan-zoom-tilt can be large consumers of power.

1.4.2 Reasons of energy waste

In WSNs, there are different forms of energy dissipation from the different unit of the sensor device. In the processing unit, the high amount of data requires a lot of energy, so minimizing the size of the data will significantly reduce the processing treatment and the time of transfer. Transmitting or receiving data demands much more energy than the other units, this makes communication subsystem is a greedy source of energy. According to [24], there is also a great amount of energy wasted in states that are useless from the application point of view, such as [25]:

- *Collision:* when a node receives more than one packet at the same time, these packets collide. All packets that cause the collision have to be discarded and the transmission of these packets is required another time which makes a waste of time and energy.
- *Overhearing*: when a sender transmits a packet, all nodes in its transmission range receive this packet even if they are not the intended destination. Thus, energy is wasted when a node receives packets that are destined to other nodes.
- *Control packet overhead*: in some protocols the overhead of the packets is much more than the data itself. So a minimal number of control packets should be used to enable data transmissions.
- *Idle listening*: it happens when a sensor node is waiting for a packet and even if it is not sure of receiving it. This mode requires a lot of energy, so it is one of the major sources of energy dissipation.
- Interference: each node located between transmission range and interference range receives a packet but cannot decode it.

1.4.3 Identifying possible energy efficiency techniques:

Since the sensor nodes are usually placed in hard to access areas, battery replacement is a complex and expensive operation almost in every WSN. That is why one of the most important WSN efficiency criteria is the network lifetime. This section is about finding and identifying common efficiency techniques which affect and extend the lifetime of WSNs. We can identify five main energy efficient techniques [24] which are:

1) ***Data reduction****:* concentrating on reducing the amount of data to be produced, treated and transferred. For example, data compression and data aggregation are the most used in such techniques.

2) ***Protocol overhead reduction****:* Some protocols have a high packet on the overhead, so the aim of this technique is to increase protocol efficiency by reducing this overhead. However, some existed techniques adapt the transmission periods according to the distance and the topology of the network.

3) ***Energy efficient routing****:* network lifetime is related on each individual components of the network, which, in its turn, depends on the energy content of batteries and power consumption in different modes: transmission, reception, idle and sleep. Furthermore, network lifetime depends on algorithms and protocols for data transfer, processing, routing and other

operations. For instance, the choice of routing protocols should be designed with the target of maximizing network lifetime by minimizing the energy consumed by the end-to-end transmission without modifying the hardware implementation of the sensor nodes.

4) ***Duty cycling****:* it is used to schedule the activity mode and the sleep mode of a sensor node. Transmitting, receiving and idle mode consume a lot of energy but only the sleep node saves the energy resources of the sensor node. Thus, the key technique for extending the sensor node battery life is the reduction in duty-cycle, by shutting down all the main components of the sensor node in the sleep mode, excepting the part which is responsible for returning from the sleep mode when needed.

5) ***Topology control***: Network topology defines the way where all the sensor nodes and the sink communicate with each other by transmitting and receiving the data. There are some many topologies in WNSs standards. So, the idea is to control the topology in such a way to maintain reduced energy consumption while preserving network connectivity and coverage.

1.5. Wireless Multimedia Sensor Network

In the previous sections, we described a typical wireless sensor network and also we discussed the different factors and elements that affect the functioning of the whole wireless sensor network, from designing and from energy consumption point of views. Hence, the following sections are dedicated to a specific type of WSN which is wireless multimedia sensor network [26].

WMSN preserves the same characteristics of a typical WSN, however, some additional changes are provided depending on its specific task.

1.5.1 WMSN and their applications:

A new technology called CMOS (Complementary Metal Oxide Semiconductor), which generally used for the manufacture of computer processors, has been used for video cameras. Using CMOS technology, image sensors can be implemented with a lens, an image sensor, and an image processing circuit on the same chip. This significantly reduces the scale and cost of image sensors. Since CMOS image quality closely follows the Charge Coupled Device (CCD) quality for low-and medium-resolution sensors, the reduction in size does not affect the quality. Moreover, CMOS sensors consume much less energy than their CCD counterparts [27], which make them suitable candidates for WMSNs.

Wireless multimedia sensor networks have found a variety of applications in numerous different fields [28] such as: battle field reconnaissance, security monitoring [29], traffic surveillance and control, automated assistance for elderly and family, health care, and environmental monitoring [30] etc. Multimedia data, including audio, images and video is typically bandwidth intensive and delay sensitive. These characteristics result in high demands on the communication and computing aspects of these systems, and thus a very high demand on energy resources.

Similar to traditional WSNs, each component in WMSNs is constrained in terms of battery, memory, processing capability, and data rate [27]. The increased traffic volume as well as the significantly higher processing requirements of encoders signifies the importance energy-efficient operation in WMSNs. Consequently, the existing resources need to be efficiently consumed for multimedia delivery.

Multimedia applications generate high volume of traffic, which require longer transmission times for battery –constrained sensor devices. While transmission is usually mitigated through in-network solutions in traditional WSNs, the extensive processing requirements of multimedia data may make these techniques unsuitable for WMSNs. Solutions for WMSNs need to guarantee the quality of service (QoS) requirements of applications while minimizing the energy consumption.

1.5.2 Structure of wireless multimedia sensor networks

Figure 1.3 presents a general wireless multimedia sensor network structure, it consists of three parts: wireless multimedia node (WMN), wireless cluster head (WCH) and a network node.

Each WMN consists of a camera or audio sensor, processing unit communication unit and power unit. Each node captures the wanted scene, called image frames, within its Field Of View (FOV). The acquired data passes through a processing unit to perform the necessary treatment to reduce the high amount of scene data.

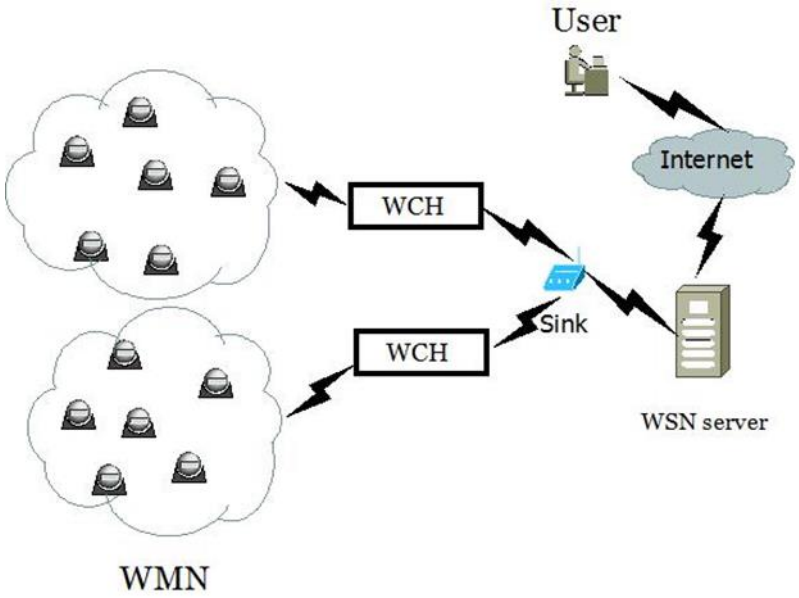

Figure.1.3. *Wireless Multimedia Sensor Networks (WMSNs) structure*

The WCHs connect a group of WMSNs and receive the data from them. Each WCH consist of a processing unit, communication unit and power unit. The Field Of View of WMNs may overlap so the WCH can reduce the unnecessary data by performing event aggregation and combination. The WNN performs the same role as for a traditional wireless sensor network and consists of a communication unit and power unit. The communication unit relays the data from node to node until it arrives at the sink. The base station or the sink gathers all the data of the network and send it to the user.

1.5.3 Characteristics of wireless multimedia sensor nodes in terms of energy consumption:

Wireless sensor networks have typically the same characteristics of a general wireless sensor network. But, since the WMSNs deals with a large amount of data, there are some additional requirements in sensing, processing and communication units. In this section, we present some characteristics of this type of sensor networks:

***Extend the battery lifetime*:** Since multimedia data contains videos, images and scalar data that consumes a lot of energy which make the battery of this sensor nodes drains quickly. Thus, an additional effort is used in the different units; from sensing to receiving the data and going through a huge and extensive processing and communication process, with the aim to conserve in battery, memory and extend the lifetime of the whole WMSNs.

High Bandwidth Demand and communication requirements:

The energy consumption in the WMSN will determine the network lifetime. The energy consumed for communication is much higher than that for sensing and computation and grows exponentially with the increase of transmission distance. Therefore it is important that the amount of transmissions and transmission distance be kept to a minimum to prolong the network lifetime and it could be possible by minimizing the amount of data to be sent [27].

To reduce the transmission distance, there are many communication schemes available in WMSN architecture such as a multi-hop short-distance communication scheme. In this scheme, a sensor node transmits data towards the sink through one or more intermediate nodes. The architecture of a multi-hop network can be organized into two types: flat and hierarchical. This process not only reduces the energy consumption for communication but also balances the traffic load and improves scalability when the network grows.

In WMSN, There are some data that needs to be delivered in real time, so, some quality of service which deals with latency and delay, reliability and quality of transmitted data must be considered.

WMSN platform: According to [31], WMSN has three categories of platform depending on their processing power and storage, which are: lightweight-class platforms, intermediate-class platforms and PDA-class platforms. Lightweight-class platforms designed with low processing power capability, small storage and are usually equipped with basic communications only. Intermediate-class platforms better than the first category in memory storage and computational processing power, but they have almost the same in communication protocols. However, PDA-class platforms are used to process high quality multimedia content and have more powerful processing capability and memory requirement and they have better communication system with a high consummation of energy.

Image and video compression: Exploiting the intraframe and interframe redundancy is absolutely necessary to reduce the amount of data to be processed and transmitted, which leads to a meaningful decrease in energy consumption. Moreover, the type of compression algorithms used, may add more computational complexity where wireless multimedia sensor networks systems do not allow it. So, the choice of a low complexity image and video compression scheme is a relevant step to take to increase the lifetime of a sensor node. We will discuss this fact in detail in chapter 2,3 and 4.

1.6. Conclusion:

In this chapter, we did a detailed study on wireless sensor networks and we exposed some necessary basics in order to better understand the problematic of this thesis.

As WSN devices are the most emerged technologies nowadays, many researchers are focusing on the evolution of these networks to be more and more used in different applications. The main burden on the development of these networks is the limited power supply and the high energy consumption. So many techniques of energy efficiency have been used in a wireless sensor networks in order to minimize the energy consumption in every single sensor node, which leads at maximizing the lifetime of the whole network.

We have presented a specific case on wireless sensor networks which is wireless multimedia sensor networks. Since this network processes high amount of data which are images and videos, not like the classic network which manipulates only scalar data, an additional effort is really necessary to be able to manage the existing energy conservation techniques and reduction the energy consumption in these networks.

In the next chapter, we will focus in image compression techniques in order to minimize the size of the data to be transmitted and gain in the network lifetime.

Chapter 2

Image compression in wireless multimedia sensor networks

2.1 Introduction

The compression process is unavoidable step for the optimization of high volume of information. The main objective of image compression is to reduce a large amount of data without sacrificing the visual representation of the original image.

This objective is achievable with the exploitation of the image redundancy. This redundancy could be spatial (correlation between pixels of one image), psycho-visual (data less perceptible to the human visual system) and spectral (spectral band). With the suppression of different sort of redundancies, compression and information loss will affects the reconstructed image quality.

In this study, we are interested in lossy image compression to achieve high compression ratios. Hence, we will focus on different compression techniques based on orthogonal transformation. The first step in such compression is the transformation, which transforms the image from a spatial domain (temporal domain) to a frequency domain. Moreover, it is like a gateway to go through a spatial domain where the coefficients are correlated to a frequency domain where the neighborhood coefficients are totally decorrelated. Thus, the significant coefficients are compacted in low frequencies.

The Discrete Cosine Transform (DCT) and the Discrete Wavelet Transform (DWT) are two transforms that are used in the well-known standards JPEG and JPEG2000 respectively. In this chapter we will focus our study on DCT and DWT based compression.We will concentrate on their characteristics in the context of WMSNs systems. In addition, a survey of research efforts to improve their energy efficiency is presented.

2.2 Image compression in wireless image sensor network

Image compression technique could be classified into two categories: lossless image compression and lossy image compression.

- Lossless image compression: It is a reversible compression. It allows a perfect reconstructed of the original image from the compressed one.
- Lossy compression: widely used in WMSNs, they allow only reconstruction of an approximation of the original image.

In general, lossless compression techniques do two steps in sequence: the first step generates a statistical model for the input data, and the second step uses this latter to map

input data to bit sequences in such a way that "probable" (e.g. frequently encountered) data will produce shorter output code than "improbable" data.

The first encoding algorithms used to produce bit sequences are the Huffman coder and the arithmetic coder. Arithmetic coding achieves compression rates close to the best possible for a particular statistical model, which is given by the information entropy, whereas Huffman coder is simpler and faster but produces poor results [33-34].

The lossy image compression techniques are divided into two categories: transform-based image compression [35]; like the DCT and the DWT, and the non transform-based algorithms such as the vectorial transformation [36] and the fractal compression [37]. In this study we will only focus on transform-based image compression.

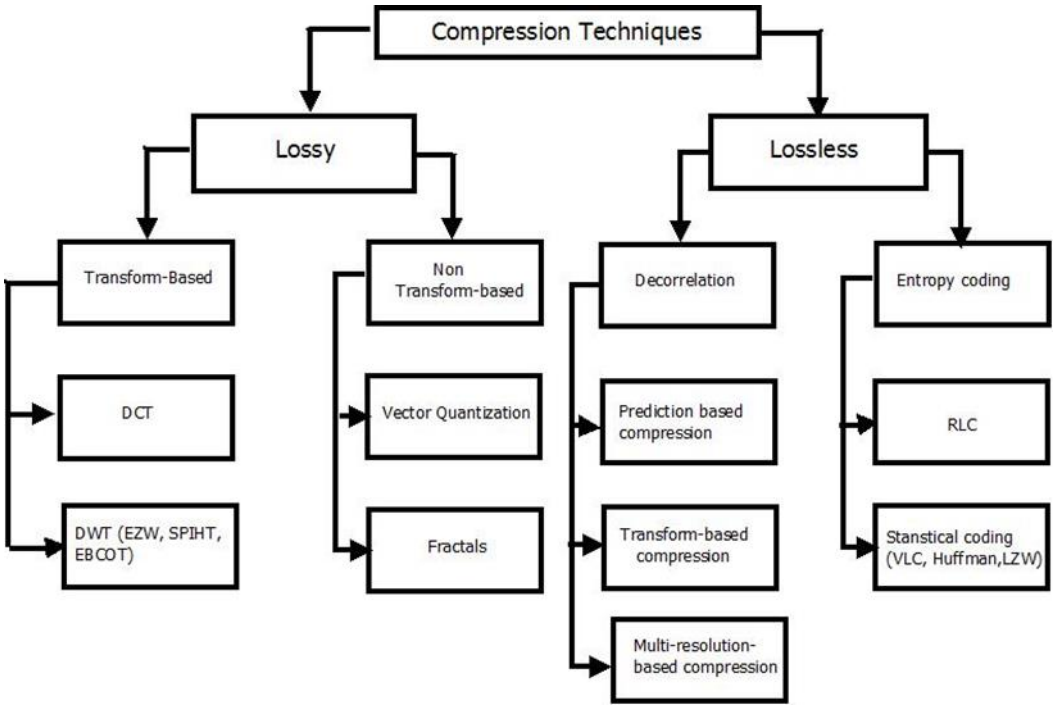

Figure2.1. Algorithm classification for image compression

The majority of studies that have been applied in scalar sensor networks supposed that the cost of computation, including data acquisition and compression is insignificant compared to the cost of communication of the same data [38]. This assumption is available only in scalar sensor networks, where the cost of compression is negligible against the cost of communication, so the compression is gainful.

In WMSNs, this assumption is not verified. The visual flux needs always compression. Actually, image compression is the perfect choice to do before transmission to gain in energy

and time. It is clear that some image compression algorithms consume a lot of time and energy than others. In general, these algorithms are used in storing, where no real time requirements is imposed. Such as, the majority of image compression algorithms: fractal compression, JPEG, JPEG 2000 requires a lot of execution time and energy. However, they give high image compression ratio when applied in traditional wired network contrarily when applied in WSNs.

2.3 Principles of image compression

Transform-based image compression has three main steps. The first one is the transformation, in this part; we pass from the pixel domain to the frequency domain in order to decorrelate image coefficients and to have energy compaction in low frequencies.

The second step is the quantization or thresholding, the quantizer reduces the output of transformation part according to psychovisual criterion. This operation provides loss of information, so, it is irreversible and targets to remove irrelevant information from the image. When lossless compression is needed, quantizer must be removed. The final stage of the encoding process of image compression is the symbol or entropy encoding. In this part, the quantified data will be reduced for transmission goals.

In order to reconstruct our image, the inverse operations will be provided in each step. The whole compression process is shown in figure 2.2.

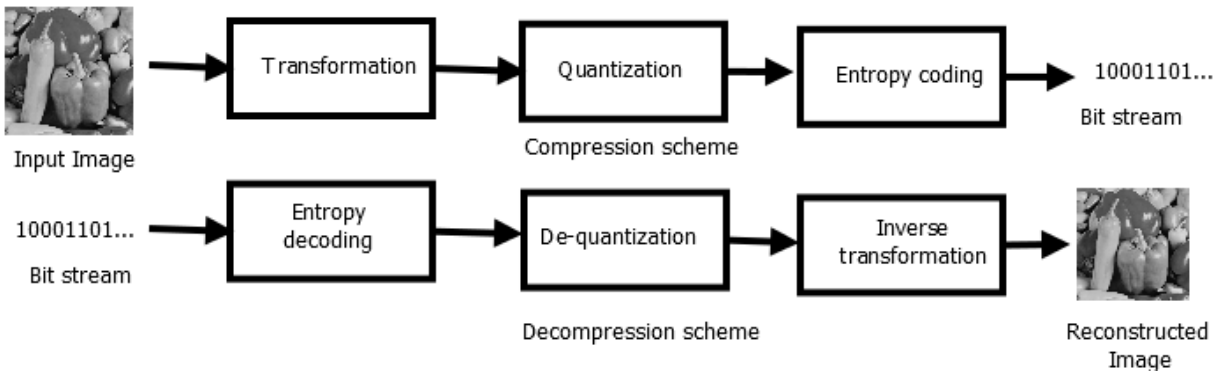

Figure.2.2. *Image compression/ decompression model*

Transformation: The transformation decorrelates the input pixels. So, the choice of the transformation is very important factor in data and image compression.

The well-known transformations used in this domain are: the Karhunen-Loeve Transform (KLT), The Discrete Fourier Transform (DFT), the Discrete Cosine Transform (DCT), the

Walsh Hadamard transform (WHT) and the Discrete Wavelet Transform (DWT). The KLT is the optimal transform that has the highest decorrelation of coefficients property; however, it has not a fast algorithm to do a real implementation. The DCT and The DWT are the widely used image compression algorithms [39].

***Quantization and thresholding*:**The quantization step provides another representation of each coefficient after the transformation step according to the quantization table. The choice of the quantization table and the threshold is a relevant factor and it must takes on consideration the human visual system (HVS), in order to obtain a better quality and a high compression ratio [39-41]. In general, a standard quantization table is used in each compression technique. This step is irreversible and generates degradation in the quality and also a loss in image information.

***Entropy encoder*:**After the quantization and thresholding, the final stage of the encoding process is the entropy encoder, which generates a fixed or variable-length code to represent the output of the quantization step. Usually the shortest code words are assigned to the most frequently occurring quantizer output values to minimize coding redundancy. For a reliable transmission, the quantified data will be reduced significantly. This operation is reversible, the most used methods are: Huffman coding [42], arithmetic coding [43] and Golomb coding [44]. According to the transformation type, the most used transformations are JPEG standard based DCT; JPEG2000 and SPIHT standards based DWT.

2.4 DCT-based compression

JPEG is the acronym of Joint Photographic expert group. It is the most popular and widely used DCT-based compression algorithm for images. It has user-adjustable compression ratio with an acceptable to a good reconstruction quality. It has lower computational complexity for widespread practical applications. Discrete cosine transform (DCT) [45] is used as the transform in the JPEG standard. According to [46] JPEG defines four modes of operations:

• *Sequential lossless mode:* It compresses the image into a single scan and the decoded image is an exact replica of the original image.

• *Sequential DCT-based mode:* It compresses the image into a single scan using DCT-based lossy compression technique. Therefore, the decoded image is an approximation of the original image. This Mode is also called as JPEG baseline mode and it is the widely used.

• *Progressive DCT-based mode:* It compresses/decompresses the image in multiple scans. Each successive scan produces better quality image.

• *Hierarchical mode:* It compresses the image at multiple resolutions for display on different devices.

In the following section, we will present sequential encoding, which is the base of the other modes. We will adopt the widely used JPEG baseline for an 8 x 8 partitioning.

***Sequential encoding*:** In JPEG compression, the image source is first partitioned into blocks of 8×8 pixels and each block is coded independently from left to right and from top to bottom [47]. After the Discrete Cosine Transform (DCT), each block of 64 DCT coefficients is uniformly quantized by a quantization table. After that, all of the quantized coefficients are ordered into a zigzag sequence, such that low-frequency coefficients are to be processed prior than high-frequency coefficients. After that, Huffman coding will be applied in order to prepare the symbols to a reliable transmission. Finally, for image reconstruction, the inverse operations will be provided in each step.

Figure 2.3 presents the different steps of JPEG standard for image compression and decompression.

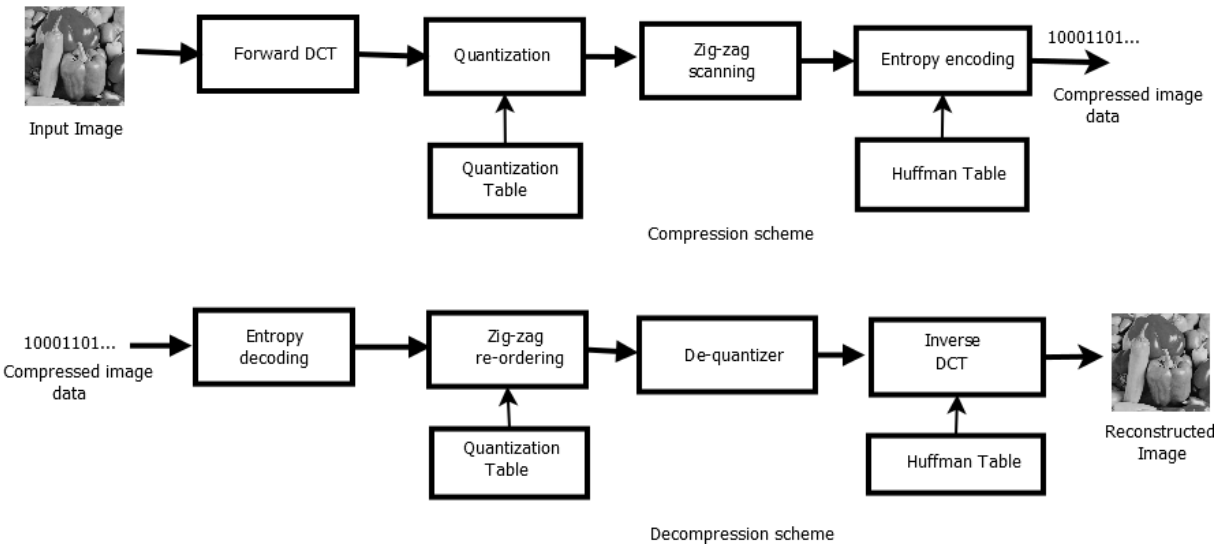

Figure 2.3: *Baseline JPEG: Compression and decompression schemes.*

2.4.1 The Discrete Cosine Transform (DCT)

A DCT represents the input data points in the form of a sum of cosine functions that are oscillating at different frequencies and magnitudes. Regarding the dimension of input data there are mainly two types of DCT: one dimensional 1D DCT and two dimensional 2D DCT. Since an image is represented as a two dimensional matrix, the 2D DCT for an $N \times N$ input sequence (x(i,j)) can be defined as follows:

$$Y(u,\upsilon) = \frac{C(\upsilon)}{2}\frac{C(u)}{2}\sum_{j=0}^{N-1}\left[\sum_{i=0}^{N-1} x(i,j)\cos\frac{(2i+1)u\pi}{2N}\right]\cos\frac{(2j+1)\upsilon\pi}{2N} \quad (2.1)$$

Where: $u\ and\ v = 0 \ldots N$ and

$$C(u) = \begin{cases} \frac{1}{\sqrt{N}} & if\ u = 0 \\ \frac{2}{\sqrt{N}} & else \end{cases} \quad (2.2)$$

In the DCT compression, almost all of the information is concentrated in a small number of the low frequency coefficients. The lowest frequency coefficient is known as Direct Components (DC) and the rest of the components are Alternative Components (AC).

To apply the forward DCT (FDCT), first the image is divided into non-overlapping 8×8 blocks in raster scan order from left to right and top-to-bottom. Then, each pixel is level shifted to convert into signed integer by subtracting 128 from each pixel.

The equation for the 2-D inverse DCT transform is given in the Eq. (2.3).

$$x(i,j) = \sum_{v=0}^{N-1}\sum_{u=0}^{N-1}\frac{C(v)}{2}\frac{C(u)}{2}Y(v,u)\cos\frac{(2i+1)u\pi}{2N}\cos\frac{(2j+1)v\pi}{2N} \quad (2.3)$$

***Preprocessing*:** For a grey scale image, the values of pixels are between 0 and 255 with a step of 1. Black is represented with 0 and white is represented with 255. It is convenient to apply the DCT in the range of -128 to 127, so, each original bloc will be leveled with a subtraction of 128 for each coefficient of the input matrix.

The DCT will be applied in each bloc after the preprocessing using the following function:

$$Y = C * X * C^t \quad (2.4)$$

Where:

X is the leveled input matrix;

C is the orthogonal matrix and C^t is the transpose;

Y is the transformed matrix.

Matrix X is multiplied by C to generate CX . So we will have the row transformation, the result will be multiplied with $C^t$to have the column transformation.

2.4.2 The quantization step

As human eye is more sensitive to low frequencies than high frequencies, the coefficients of the quantization matrix depend of the chosen quality factors. If the quality factor is very small so the image quality is low and the compression rate is very high. However, if this factor is high, so the image quality is good and the compression rate is low.

The following quantization matrix is the standard table used in JPEG norm:

$$\boldsymbol{Q} = \begin{bmatrix} \mathbf{16} & \mathbf{11} & \mathbf{10} & \mathbf{16} & \mathbf{24} & \mathbf{40} & \mathbf{51} & \mathbf{61} \\ \mathbf{12} & \mathbf{12} & \mathbf{14} & \mathbf{19} & \mathbf{26} & \mathbf{58} & \mathbf{60} & \mathbf{55} \\ \mathbf{14} & \mathbf{13} & \mathbf{16} & \mathbf{24} & \mathbf{40} & \mathbf{57} & \mathbf{69} & \mathbf{56} \\ \mathbf{14} & \mathbf{17} & \mathbf{22} & \mathbf{29} & \mathbf{51} & \mathbf{87} & \mathbf{80} & \mathbf{62} \\ \mathbf{18} & \mathbf{22} & \mathbf{37} & \mathbf{56} & \mathbf{68} & \mathbf{109} & \mathbf{103} & \mathbf{77} \\ \mathbf{24} & \mathbf{35} & \mathbf{55} & \mathbf{64} & \mathbf{81} & \mathbf{104} & \mathbf{113} & \mathbf{92} \\ \mathbf{49} & \mathbf{64} & \mathbf{78} & \mathbf{87} & \mathbf{103} & \mathbf{121} & \mathbf{120} & \mathbf{101} \\ \mathbf{72} & \mathbf{92} & \mathbf{95} & \mathbf{98} & \mathbf{112} & \mathbf{100} & \mathbf{103} & \mathbf{99} \end{bmatrix}$$

After transformation, the transformed coefficients will be quantized. This step is primarily responsible for the loss of information and hence it introduces distortion in the reconstructed image. Each 64 DCT coefficients are uniformly quantized according to the following formula:

$$Y_Q(u,v) = Round\left(\frac{Y(u,v)}{Q(u,v)}\right) \qquad (2.5)$$

Where $Y(u,v)$ are the DCT coefficients and $Q(u,v)$ is the quantization table. In the case of color images, JPEG standard defines two quantization matrices for luminance and chrominance planes. These two quantization matrices have been designed based on the psycho visual experiments by Lohsceller [48] to determine the visibility threshold for 2-D basis functions. These matrices are best suited for natural images with 8-bit precision. Quality

of the reconstructed image can be controlled by scaling the matrices. Further compression can be achieved by applying appropriate scaling factor. In order to reconstruct the output data, the rescaling and the de-quantization should be performed on the compressed image data.

2.4.3 Zigzag Scanning

After the transformation and quantization over an 8 × 8 image sub-blocks, the new 8 × 8 sub-block shall be reordered in zigzag scan into a linear array as shown in Figure 2.4. The first coefficient is the DC coefficient and the other 63 coefficients are AC coefficients. The DC coefficient contains lot of energy; hence it is usually of much larger value than AC coefficients. Since there is a very close relation between the DC coefficients of adjacent blocks, the DC coefficients are differentially encoded. The scan is in a zigzag form in order to provide the scan in rows and columns as well.

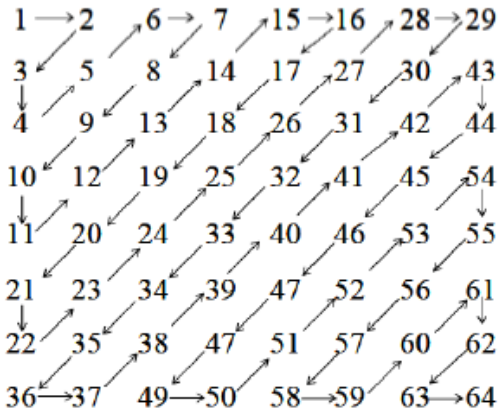

Figure 2.4. *Zigzag scanning*

The entropy coding process consists of Huffman coding tables as recommended in JPEG standard [47]. These tables are stored as header information during the compression process so that it is possible to uniquely decode the coefficients during decompression process.

2.4.4 Entropy Coding

The quantized DCT coefficients are integers and must be entropy coded for transmission or storage. The baseline system uses Huffman coding. Because the DC coefficients of neighboring blocks are correlated, further compression is achieved by coding the DC differences. The quantized AC coefficients are Huffman coded using run-length/amplitude pairs.

2.4.5 DCT-based compression and wireless sensor networks:

JPEG is the most recommended standard in image compression domain, and the DCT is the transformation used in this standard. This transformation has high compaction of the coefficients in low frequencies, it is less complicated than the DWT, easy to implement and it gives high compression ratios. However, it has blocking artifacts phenomena and fake contouring in high compression ratios.

Despite all this advantages of the DCT, it still not possible to use it in the constraints of wireless image sensor networks. Furthermore, in JPEG standard, the transformation (DCT) is the part that consumes most of energy, about 60% of the whole chain [49]. This consummation not really favorable in wireless image sensor networks. So many researchers attempt to reduce the energy consumption due to this step. Some of the works are based on:

***Algorithmic level*:** This is based on reducing the number of operations that requires a lot of energy, like the multiplication operations. Loeffler and al [50] had demonstrated that the minimum number for the calculation of the DCT 8 points is 11 multiplications and 28 additions. So many algorithms exist in the literature attempt to reduce the arithmetic complexity of the DCT [51-53], by converting the multiplication operations to simple operations, such as additions and shifts operations.

These converted operations are some kind of approximation and they degrade the quality of the reconstructed image. However, these systems provide a fast implementation and require less computational resources compared to the exact DCT.

***Scheme level*:** many techniques [53-56] have been used the most important of them are:

- Some schemes that use the parallelism and pipeline of the DCT 2D: it consists on using the row/column decomposition based on two 1 D processors and an intermediate buffer memory using the parallelism concept. The proposed scheme generates a parallel processing for the arithmetic units. Hence, according to [57], this will provide a reduction in complexity for the both computation and interne memory, and allows a high rate of compression.
- In processor architectures operations using float data types are expensive and energy consuming. So, the idea consists of using a DCT with an integer point instead of floating point. Most hardware platforms, instead of having devoted floating point for hardware units, they use simple and low-cost fixed-point arithmetic units. According

to an example in [57]:JPEG coding of QCIF format grey scale image at 1 bit per pixel (bpp), using a Strong ARM SA1110 processor requires 2.87 mJ with the fixed-point (integer) DCT. The same operation requires 22 mJ using the floating point DCT. This is a justification for the use of the intger DCT in image sensor networks.

- Another method used for the reduction of the elements to be processed is the Distributed Arithmetic (DA). It consists on replace the constants multipliers with a lookup table and accumulators in order to reduce the implementation complexity [58].

2.5 DWT-based compression

2.5.1 The Discrete Wavelet Transform (DWT)

JPEG2000 is an image compression standard based on the discrete wavelet transform. The DWT is a multi-resolution technique that proves its efficiency in image compression field. The property of multiresolution is one of the properties that are very important on the DWT. It represents an image as a sum of wavelet functions, known as *wavelets*, with different location and scale [59].The input data is passed through set of low pass and high pass filters. In case of 2-D DWT, the input data is passed through set of both low pass and high pass filter in two directions, both rows and columns. The data passed through the low pass are the approximations, and the data passed through the high pass are the details. The outputs of these filter banks are then down sampled by 2 in each direction as in case of 1-D DWT. At the end, we will obtain a set four coefficients which are: Low Low (LL), High Low (HL) which contain vertical elements, Low High (LH) which contain horizontal elements and High High (HH) which contain diagonal elements. Figure 2.5 gives in detail the whole process.

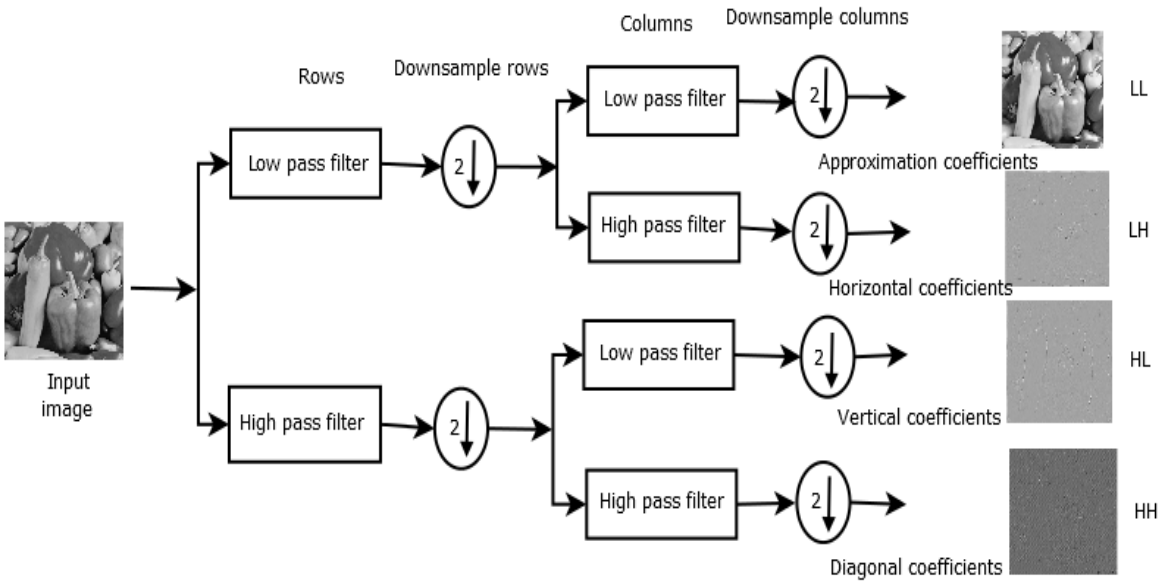

Figure 2.5. *Block diagram of 2-D forward DWT*

In DWT reconstruction, input data can be achieved in multiple resolutions [59] by decomposing the LL coefficient further for different levels as shown in Figure 2.5. In order to reconstruct the output data, the compressed data is up-sampled by a factor of 2. The signal is further passed through the same set of high pass and low pass filter in both rows and columns. The entire reconstruction procedure is shown in Figure 2.6.

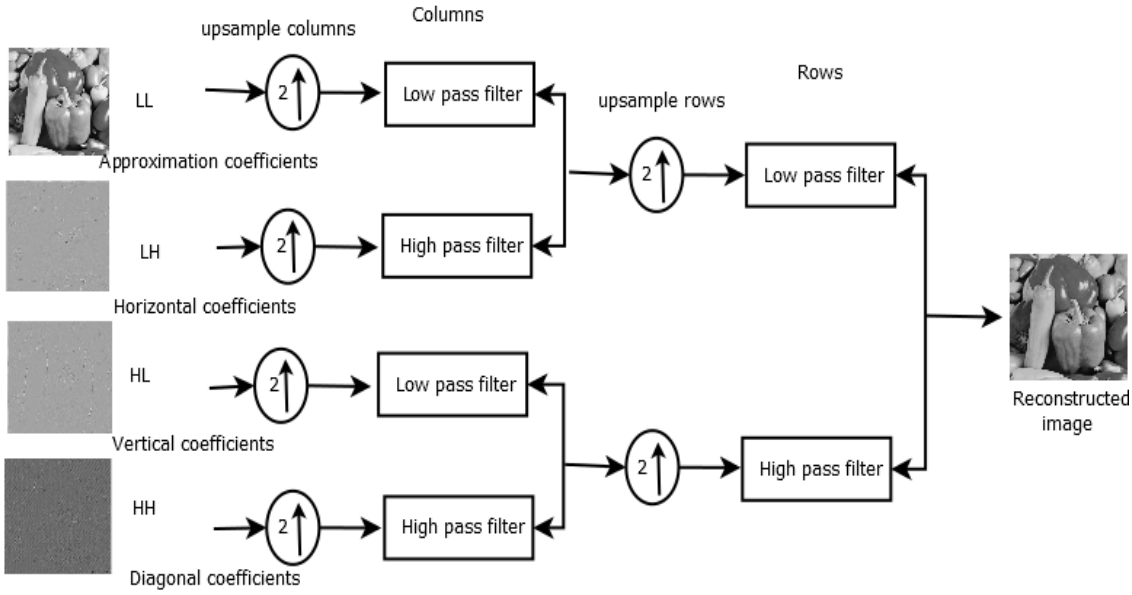

Figure.2.6. *Block diagram of 2 dimensional inverse DWT*

Discrete Wavelet Transform (DWT) is an effective transform that provides significantly higher compression efficiency than DCT at higher compression ratio. However, DWT is so complicated in its implementation and requires a lot of energy compared to the DCT. Thus, several researchers focus on reducing its complexity and memory requirement. According to [60], the lifting scheme is an algorithm that calculates the DWT efficiently because it uses less filter coefficients which provides an easy implementation and memory reduction of the DWT. The two best-known compression algorithms that uses the DWT are "Set Partitioning in Hierarchical Trees" (SPIHT) and JPEG2000.

2.5.2 Set Partitioning in Hierarchical Tree (SPIHT)

Set partitioning in hierarchical trees (SPIHT) is an image compression algorithm that exploits the similarities across the sub-bands in a wavelet decomposition of an image. Researchers showed that the images obtained with algorithms based on the wavelet transform provide a very good visual quality. It was shown that even simple coding methods produced good results when combined with wavelets. Since the SPIHT belongs to a more sophisticated coding that is based on the DWT, it is clear that this fact increase the efficiency of SPIHT.

In SPIHT, an image is first transformed into the wavelet domain where the quad-tree structure is explored by a bitplane coding algorithm. The inter-band wavelet correlation is reduced by two pass filters: the sorting pass and the refinement pass. The output of these two filters is a bit-stream with descending importance order.

This compression is very fast and has high compression quality. In addition, the storage of quad-tree structure and significant information requires many memory resources which cause a complex implementation.

2.5.3 Joint Photographic Expert Group 2000 (JPEG2000)

As we mentioned in DWT section, the JPEG2000 is a well-known standard based on the DWT. In JPEG2000, an image is divided into rectangular regions of the image that are called tiles, which are transformed and codded independently. This division is advantageous that the decoder will need less memory to decode the image, however, the quality of the reconstructed image decreases. The wavelet transforms are implemented by the lifting scheme or by convolution. After the wavelet transform, the coefficients are quantized and coded using the Embedded Block Coding with Optimal Truncation (EBCOT).

2.5.4 DWT-based compression and wireless sensor network:

JPEG2000 and SPIHT are two standards of image compression that use the DWT. JPEG2000 provides slightly higher compression quality than SPIHT. However, JPEG2000 uses a multi-layer coding procedure which makes it more complex and requires more computational resources and memory [60]. Furthermore, the optimization process adds a supplement to the computational requirements. Since the SPIHT provides a high compression ratio with relatively low complexity [61], so it is the best energy-efficient DWT based compression.

Many state-of-art wavelet-based image coding algorithms have been adapted in the context of WMSNs [62-63]. However, the traditional DWT is implemented with memory intensive and time consuming algorithms and therefore has very high system resource requirements. Hence, it is not suitable for multimedia applications on memory-constrained portable devices, such as digital cameras and sensor nodes in WMSNs. Recently in [64] wavelet-based image coder with low memory requirements and low complexity that preserves the compression efficiency is proposed. This encoder employs a new type of wavelet known as the Fractional Wavelet Filter (FrWF). To the best of our knowledge, only limited efforts have been made to minimize the overall memory and complexity requirements of image codecs based on DWT.

2.6 Conclusion

In this chapter, we have done a survey on image compression techniques; however, we have focused on some well-known standards like JPEG, JPEG2000 and SPIHT. We studied in this chapter their performances in terms of decompressed image quality and energy consumption, in order to find out the best method that response to the exigence of wireless multimedia sensor networks.

From all above study, we conclude that the DCT based compression is the most suitable transform to apply in WMSN because of its relatively low complexity. However, its complexity must be reduced more and more in order to save in time and energy and increase the lifetime of the sensor node.

In the next chapter, we will focus on low complexity DCT approximation and other low complexity techniques. Hence, a technical study and performances evaluation will be processed.

Chapter 3

Proposed low complexity image compressions

3.1 Introduction

Reducing the algorithmic complexity of image compression techniques is a great challenge in wireless image sensor networks (WISNs) [65-68]. These WISNs are often under constraint of energy autonomy. Many image compression standards such as JPEG and JPEG2000 are not suitable for implementation in WISN, as reported in [69]. Such standards do not guarantee energy savings due to their high computational complexity.

As we mentioned in the previous chapters, the transformation step such as discrete cosine transform (DCT) and discrete Tchebichef transform (DTT) consumes more than 60% of the computational requirements in JPEG standard for image compression [70]. Therefore, significant improvements in speed and energy with JPEG technique can be obtained; by reducing the computational complexity of the transform and that what we focused on it in this chapter. So we have proposed a low complexity image compression schemes based on the DCT and/or the DTT in order to more reduce the arithmetic complexity and gain in time and energy consumption.

Since these algorithms are floating-point and they are implemented with high algorithmic complexity and memory intensive. Therefore, they consume large system resources. In particular, those requirements pose a serious limitation on multimedia applications in resource-constrained systems, such as wireless multimedia sensor networks (WMSNs). Moreover, some researches turn out their focus to the Discrete Tchebichef Transform (DTT), as an alternative method of the DCT. Despite its good energy compaction property, low algorithmic complexity and low memory requirements, the DTT is potentially unexploited in the literature. So, they recently tried to study and evaluate the areas where the integer DTT outperforms the DCT, in order to use it in the field of image and video compression. This transformation has been already used for several applications in image processing such as artifacts measurement [71], image analysis [72] and recently in image and video coding [73-74].

In this chapter, we will propose new DCTs [75-76] to more reduce the arithmetic complexity and also to maintain a good trade-off quality/complexity, which is suitable for resource constrained low-power sensors nodes. In the other hand, we will prove that the DTT is a useful tool in image and video compression by proposing a Pruned Discrete Tchebichef Transform (P-DTT)[77] that exhibits low computational complexity and high image compression performance.

Simulation performances will be in terms of image quality objective and subjective, and also in terms of number of operations used by each method, execution time and energy consumption.

3.2 Properties of the DCT

The following section presents some properties of the DCT that are extremely important, the most used of them are:

3.2.1 Energy compaction

Efficiency of a transform scheme especially in applications such as image and video compression can be directly measured by its ability to pack input energy into as few coefficients as possible. This allows the quantizer to discard coefficients with relatively small amplitudes without introducing visual distortion in the reconstructed image.

The Karhunen-Loève transform (KLT) presents the optimal transform that provides the perfect representation in terms of energy compaction and decorrelation of coefficients [53]. However, the KLT is data dependent, so its computational complexity is relatively high preventing its usage in typical video processing applications. The energy compaction performance of DCT approaches that of the KLT for first-order Markov signals such as images, which makes the DCT very useful tool in image processing especially in image compression.

3.2.2 Separability

The 2-D DCT transform given by equation (2.1) can be separated in row-column transformation. However, the column transformation is represented as follows:

$$Y(u,\upsilon) = \frac{C(\upsilon)}{2}\sum_{j=0}^{N-1} y(u,j)\cos\frac{(2j+1)\upsilon\pi}{2N} \tag{3.1}$$

Where $y(u,j)$ is the row transformation. This transformation is represented as follows:

$$y(u,j) = \frac{C(u)}{2}\sum_{i=0}^{N-1} x(i,j)\cos\frac{(2i+1)u\pi}{2N} \tag{3.2}$$

Hence, the 2-D transform is separable and therefore equations (3.1) and (3.2) can be computed by two successive 1-D transforms applied row-wise and column-wise on the 2-D input data array. This operation can be described in matrix notation as [78]:

$$Y = (C.(C.X)^t)^t \tag{3.3}$$

Where **C** is the $M \times N$ transformation matrix.

3.2.3 Orthogonality

The DCT transformation matrix C is invertible and its inverse denoted as C^{-1} follows the relationship $C^{-1} = C^t$. Therefore the inverse transform exists and is computed as,

$$X = ((C^t Y).C)^t \tag{3.4}$$

3.3 Assessment criteria

In this thesis, we perform our evaluations concerning the image quality in terms of MSE, PSNR and SSIM. And we evaluate the complexity in terms of number of operations, execution time and energy consumption.

3.3.1 Image quality

To evaluate the performance of the proposed transforms in image compression, we used it as part of JPEG chain. This chain includes standard quantization table and Huffman encoder that are given in the JPEG standard [79]. For this purpose, we considered a variety of 512×512 8-bit standard grayscale images taken from [80]. This set contains low-frequency, medium frequency and high frequency images. In fact, the image type has an effect on compression performance and energy compaction property ensured by the DCT. Thus, the result obtained by the same compression algorithm varies depending on the image used. So, we use a variety of images to guarantee that our results are robust. Some typical test images are shown in Figure. 3.1.

Figure.3.1. *Typical standard test images used in the simulation*

Removal of irrelevant visual information may lead to a loss of real or quantitative image information. Two types of criteria can be used to quantify loss of information:

• *Objective fidelity criteria:* Information loss is expressed as a mathematical function of the input and output of the compression process. The image quality after decompression is

measured using Peak Signal to Noise Ratio (PSNR) and Mean Square Error (MSE) metrics. The MSE and PSNR are calculated using equation (3.5) and equation (3.6) respectively:

$$MSE = \frac{1}{M \times N} \sum_{i}^{M} \sum_{j}^{N} (A_{ij} - B_{ij})^2 \tag{3.5}$$

Where, MSE denotes the mean squared error between the original (A_{ij}) and the reconstructed images (B_{ij}). $M \times N$ is the image size.

$$PSNR = 10 \log_{10} (\frac{d^2}{MSE}) \tag{3.6}$$

Where d is the maximum signal amplitude. In general, in the case of an 8 bit per pixel (bpp) image, $d = 255$.

Though these image metrics in equation (3.5) and equation (3.6) are used extensively for evaluating the quality of the reconstructed image, but these metrics do not take the visual perception system into account. So, we used another metric called Structural SIMilarity Index (SSIM) which considered image degradation as perceived change in structural information rather than perceive errors in PSNR or MSE [81]. SSIM is expressed as:

$$SSIM(A, B) = \frac{(2\mu_A\mu_B + c_1)(2\sigma_{AB} + c_2)}{(\mu_A^2 + \mu_B^2 + c_1)(\sigma_A^2 + \sigma_B^2 + c_2)} \tag{3.7}$$

Where,

A and B are the reference and distorted images;

μ_A, μ_B = mean intensities of original data A and reconstructed data B;

σ_A, σ_B = standard deviation of original data A and reconstructed data B;

c_1, c_2 = constant. The standard value of c_1 and c_2 are 0.01 and 0.03 respectively [81].

The mean intensity can be calculated as below.

$$\mu = \frac{1}{N} \sum_{i=1}^{N} x_i \tag{3.8}$$

The standard deviation is mathematically represented as:

$$\sigma = \sqrt{\frac{1}{N} \sum_{i=1}^{N} (x_i - \mu)^2} \tag{3.9}$$

And

$$\sigma_{AB} = \frac{1}{N-1}\sum_{i=1}^{N}(A_i - \mu_A)(B_i - u_B) \quad (3.10)$$

If A and B are identical then SSIM=1. For highly uncorrelated case SSIM = -1.

• *Subjective fidelity criteria:* In some cases the objective quality assessment criteria does not give us real information about the quality of the reconstructed images. So, we must use the human eyes as a subjective analysis on the reconstructed images, with the focus on the difference between the reconstructed and the original one.

3.3.2 Complexity assessment:

3.3.2.1 Number of operations:

The computational complexity of fast DCT algorithms is generally expressed as the number of Additions, Shifts and Multiplication operations required, as it is shown in [66-68], [82-87]and [88]. These operations concern the high-level algorithm used.

In our proposed transformations [75-77], we adopt the row-column method presented in Figure. 3.2 and we used the following formula for the calculation of the number of additions and shifts operations for 2D.

$$AC_{2-D}(N) = (N+8) \times A_{1-D}(N) \quad (3.11)$$

Where:

$AC_{1-D}(N)$ is the number of arithmetic complexity required to compute the 1-D transform for a bloc of N=8.

However, for the calculation of the pruned version used in our proposed methods, we used the following formula:

$$AC_{2-D}(L) = (L+8) \times AC_{1-D}(L) \quad (3.12)$$

Where :

$AC_{1-D}(L)$ is the number of arithmetic complexity required to compute L-pruned 1-D transform. L is the submatrix of size $L \times L$ $(L < 8)$to make the pruned version.

3.3.2.2 Execution time and energy consumption

To evaluate the energy consumption of the transforms in WSN node we have two methods: the first by WinAVR software and the second by mathematical model.

- **Simulation using WinAVR software**

The main focus in resource constrained wireless sensor networks is the reduction of energy consumption. To further investigate the capabilities of the proposed transform and its performance, we assess the energy efficiency of the proposed transforms in the context of WSNs.

We perform a simulation using WinAVR software similar to that in [66-68]. For this purpose, we adopt the well-known Atmel Atmega128L in [89], with an active power consumption of 23 mW at 8 MHZ, as the target platform. This latter is the microcontroller embedded in Mica2 and MicaZ wireless sensor nodes [27],[90-91].

We take the computations cycles required by the transform from the AVR simulator. Thus, we can derive the execution time (speed) and energy consumption according to the relations below:

$$T = C / F \tag{3.13}$$

$$E = T \times P \tag{3.14}$$

Where, C is the number of cycles, F is the frequency and P is the active power consumption.

- **Mathematical Model**

In addition, in a typical WMSNs node, the energy consumption is directly proportional to the number of operations that are needed by the compression algorithms of that node [92-94]. Hence, to evaluate the energy consumption of the proposed transform we developed a simple model based upon the arithmetic complexity of each transform. That methodology is adopted in many works in WSNs literature [95]**.**

Assuming that the input image size is M by N pixels then the energy spent by the transform the energy consumption could be calculated according to the following formulas:

$$\mathrm{E}_{M\times N}(\mathrm{L}) = \frac{M\times N}{8\times 8} \times E_{8\times 8}. \tag{3.15}$$

$E_{8\times 8}(\mathrm{L})$, the energy spent by the transforms for an 8x8 bloc**,** is given by:

$$E_{8\times 8}(method) = \boldsymbol{A}\cdot\boldsymbol{\varepsilon_{Add}} + \boldsymbol{B}\cdot\boldsymbol{\varepsilon_{Shift}} + \boldsymbol{C}\cdot\boldsymbol{\varepsilon_{Mult}} \tag{3.16}$$

Where

A, B *and* C are the 2D number of operations for additions, shifts and multiplications operations respectively.

ε_{Add}, ε_{Shift} and ε_{Mul} represent the energy consumption respectively for Add, Shift and Mul operations over one-pixel.

3.4 2-D DCT architectures

3.4.1 Adopted DCT architecture:

The forward and inverse 2D DCT allow the input data to go from the bi-dimensional spatial domain to the bi-dimensional frequency domain and vice versa. For an $N \times N$ input matrix the 2D DCT is calculated according to the formula 2.4. The 1D DCT has been widely studied in the past, for example by Loeffler in 1970 [50] and by Chen in 1980 [98]. At that time, the challenge was to realize the transform in a very tiny space in order to use a small space of the silicium chip and minimize the price of the implementation. Nowadays with the technology evolution, the requirements have changed; researchers focus more in speed, power reduction and flexibility maintaining in this same time an acceptable surface. For this reasons, we have used the algorithm of Loeffler which is the more economic in surface and we have used the row-column architecture for an efficient realization of the 2D DCT.

The tremendous number of operations used for a high numbers of N has led the researchers to divide the bloc matrix into small sizes (2×2, $4 \times 4, 8 \times 8$ *or* 16×16). For an input image with the size of $N \times N$, we do the previous division and after that we use the concept of row-column decomposition, which it consists on applying the 1D DCT for each row followed by the 1D DCT for columns; according to the formulas 3.1 and 3.2 respectively and as it is shown in Figure 3.2.

In our study we adopt this architecture for the realization of the DCT because it is the most adapted for a material implementation of the 2D DCT.

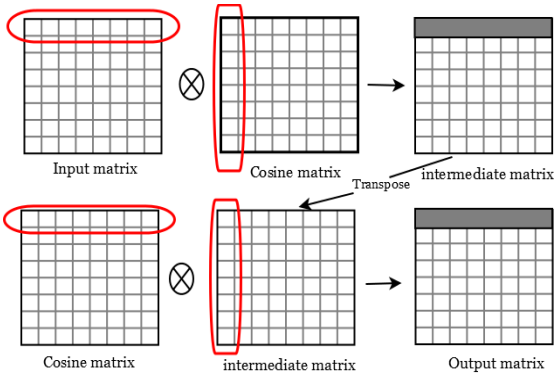

Figure.3.2. *Row-column decomposition*

The implementation of this architecture is composed with three steps. In the first step, we use the DCT which will be applied in each row vector of the input matrix. In the second step, the obtained result is memorized in a temporary buffer in order to perform the transpose on the obtained matrix. In the final stage, the 1D DCT is applied in each column of the buffer memory.

3.4.2 Pruned 2D DCT:

Generally, in image compression, image is divided into 8x8 blocks. The 2-D transform that correspond to each block $X_{8\times8}$ is expressed by:

$$Y_{8\times8} = C_{8\times8} \cdot X_{8\times8} \cdot C_{8\times8}^{t} = D_{8\times8}(T_{8\times8} \cdot X_{8\times8} \cdot C_{8\times8}^{t})D_{8\times8}^{t} \quad (3.17)$$

The inverse transform is giving by:

$$X_{8\times8} = C_{8\times8}^{t} \cdot Y_{8\times8} \cdot C_{8\times8} = T_{8\times8}^{t}(D_{8\times8}.Y_{8\times8}.D_{8\times8})T_{8\times8} \quad (3.18)$$

Where the adjustment matrix $D_{8\times8}$ can be integrated [85] into the quantisation step; therefore it does not introduce any computational overhead.

For the aim of reducing the arithmetic complexity, we have based in our study on the pruned version [96-97], which it consists on only computing the top left sub-matrix of size $L \times L$ (where $L < 8$) which contains most of the block energy as it is shown in Figure.3.3

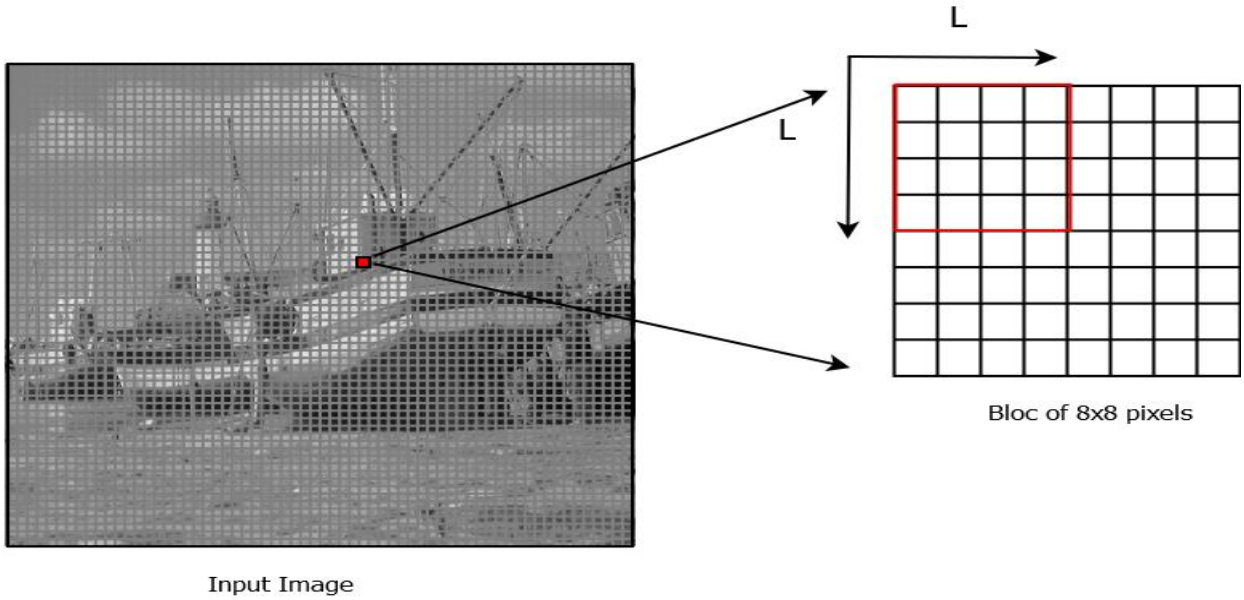

Figure 3.3. *Pruned method adopted in the proposed transforms*

Then the *L*-pruned 2-D transform is expressed by:

$$\mathrm{Y_{L\times L}} = \mathrm{C_{L\times 8}} \cdot \mathrm{X_{8\times 8}} \cdot \mathrm{C^{t}_{8\times L}} \tag{3.19}$$

Where $C_{L\times 8}$ is the *L*-pruned transformation matrix. It is given as follows:

$$\mathrm{C_{L\times 8}} = \mathrm{D_{L\times L}} \cdot \mathrm{T_{L\times 8}} \tag{3.20}$$

$D_{L\times L}$ and $T_{L\times 8}$ are the pruned versions of $D_{8\times 8}$ and $T_{8\times 8}$, respectively. Those two matrices are given as:

$$T_{L\times 8} = \begin{bmatrix} T_{0,0} & T_{0,1} & \cdots & T_{0,7} \\ T_{1,0} & T_{1,1} & \cdots & T_{1,7} \\ \vdots & \vdots & \ddots & \vdots \\ T_{L-1,0} & T_{L,1} & \cdots & T_{L-1,7} \end{bmatrix} \tag{3.21}$$

$$\mathrm{D_{L\times L}} = \mathrm{diag}(\mathrm{D_{0,0}}, \mathrm{D_{1,1}}, \dots, \mathrm{D_{L-1,L-1}}) \tag{3.22}$$

Note that $C_{L\times 8}$ is a semi-orthogonal matrix.

Simulations on several test images show that: within 8×8 blocks most of the energy is compacted in the 4×4 low frequency coefficients.

3.5 Literature review on DCT fast algorithms

Energy consumption is a critical problem affecting the lifetime of wireless image sensor networks (WISNs). In such systems, images are usually compressed using JPEG standard to save energy during transmission. And since DCT transformation is the most computationally intensive part in the JPEG technique, several approximations techniques have been proposed to further decrease the energy consumption due to this step.

Several works that aims to decrease the computational complexity of the exact DCT have been suggested in the literature, such as in [50] and [99-102]. However, these fast algorithms of the exact DCT have almost reached the theoretical limit of the complexity as reported in [102]. So, there is a little scope for major improvements by means of standard methods. For the case of 8-point DCT such complexity consists of 11 multiplications and 29 additions which are achieved by Loeffler algorithm presented in [50]. The Multiplication operations have always been the relevant problem to be solved. Indeed, most of the recent implementations of transforms employ integer approximations to avoid these multiplications [82].

In this scenario, several integer DCT approximations have been proposed for image and video coding and compression [83-86]. Haweel in [83], propose a signed DCT (SDCT) which applied a signed integer functions to the DCT matrix. The SDCT requires the same complexity as Walsh Hadamard Transform (WHT), 24 additions, and have good image compression performances. In contrast it lacks of orthogonality. The authors in [84] proposed a biorthogonal transform (BinDCT) which are good approximation of the DCT. The 1D BinDCT requires 31 additions and 14 shifts operations. Cintra et al in [85] proposed a rounded DCT (RDCT) based on integer functions. The RDCT requires 22 additions with good image compression properties. Bayer et al in [86] proposed a modified rounded DCT (MRDCT) based upon RDCT which requires 14 additions but the reduction of the complexity comes at the cost of significant decrease of Peak signal to noise ratio (PSNR). Bouguezel et al in [87] and [103-106] have proposed a series of DCT approximations. The most recent of this series is the Binary DCT (BDCT) which requires 24 additions and has a competitive image compression performance as RDCT. D Vaithiyanathan et al in [107-108] proposed a series of 8 by 8 transform matrices. The transformation in [107] is claimed to be the most efficient and requires only 12 additions. The problem with this transformation is the lack of orthogonality and the low energy compaction that involve low compression efficiency. Indeed, an orthogonal transformation ensures the decorrelation of coefficients, preserves the energy and does not amplify the noise. While a good energy compaction, transforms pack more energy into less number of coefficients. This, leads to a higher compression rate and consequently a lower bit rate.

In image compression applications [103] high-frequency DCT coefficients are often zeroed by the quantization process. To this end, only significant coefficients of DCT will be calculated. This can reduce the computational demands and memory resources considerably. This method is called pruning [104-105] and was originally applied to the discrete Fourier transform (DFT) in [106]. All above approximations reduce the computational complexity of the DCT, leading to high speed realizations, low-energy consumption, and hence ensuring an adequate numerical accuracy.

Many approximations have been reported in the literature to minimize the computational complexity of the DCT. These DCT approximations can be classified into two categories: The first replaces the original floating point transform with an integer low accuracy, such as in [82-87] The second is a pruned approach, see [66-68], [96] and [97], which reduces the

computation of the DCT by computing only the significant subset of 2-D DCT coefficients of size L×L (where L <8) which contains most of the block energy.

For pruning to be effective, good transformations must be considered. So we have made a comparison between several 8-point DCT approximations available in literature in terms of PSNR, MSE metrics and computational complexity. We chose popular transform for the comparison and the recent transform from the Bouguezel et al and D Vaithiyanathan et al series. Results illustrated in Figure. 3.4 and Table 3.1 show that the RDCT presented in [85] gives the best tradeoff quality/complexity. Consequently the proposed method is based upon this latter.

Method	**Add**	**Shifts**	**Mul**
	1D / 2D	**1D / 2D**	**1D/2D**
Transform in [107]	12 / 192	0	0
MRDCT [86]	14 / 224	0	0
RDCT [85]	22 / 352	0	0
BDCT [87]	24 / 384	0	0
SDCT [82]	24 / 384	0	0
BinDCT [84]	36 / 576	17 / 272	0
Loeffler [50]	29 / 464	0	11 / 176

Table.3.1: *Computational complexity of different DCT approximations.*

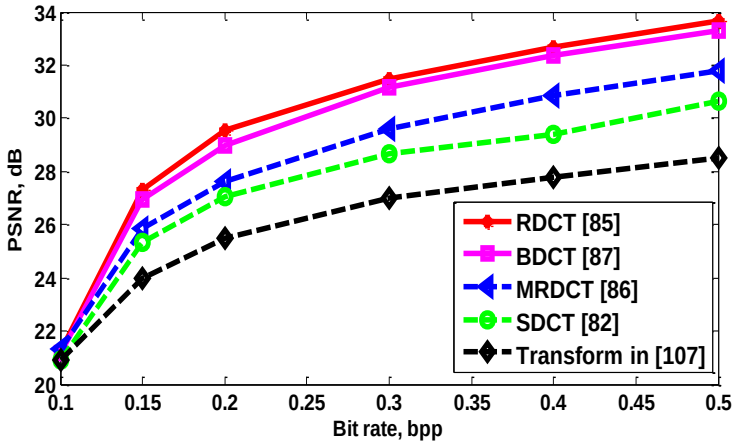

(a)

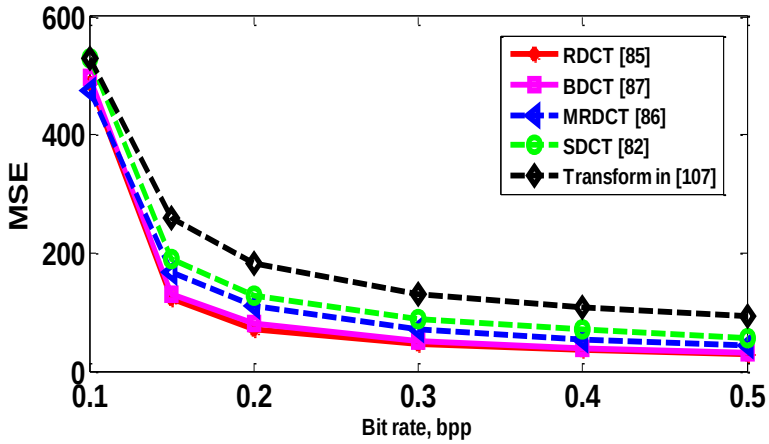

(b)

Figure 3.4. *Quality measures depending on compression ratio for different DCT approximations. Results are given for Lena image. (a) PSNR , (b) MSE.*

3.6 Proposed methods

In this thesis, we have proposed two DCTs approximations and one DTT approximation. In the following sections, we will present the mathematical concept of these proposed methods as well as simulations results in terms of image quality and energy consumption.

3.6.1 First proposed DCT approximation

3.6.1.1 Mathematical concept:

The RDCT developed in [85] presents a good energy compaction property which leads to high performances in image compression. It consists in applying round operator to the standard DCT matrix in order to obtain its entries in the integer set $\{-1, 0, +1\}$ which implies low computational complexity. The RDCT has the following transformation matrix:

$$T_{8\times8} = \begin{bmatrix} 1 & 1 & 1 & 1 & 1 & 1 & 1 & 1 \\ 1 & 1 & 1 & 0 & 0 & -1 & -1 & -1 \\ 1 & 0 & 0 & -1 & -1 & 0 & 0 & 1 \\ 1 & 0 & -1 & -1 & 1 & 1 & 0 & -1 \\ 1 & -1 & -1 & 1 & 1 & -1 & -1 & 1 \\ 1 & -1 & 0 & 1 & -1 & 0 & 1 & -1 \\ 0 & -1 & 1 & 0 & 0 & 1 & -1 & 0 \\ 0 & -1 & 1 & -1 & 1 & -1 & 1 & 0 \end{bmatrix} \quad (3.23)$$

With an 8×8 image block, DCT concentrate on average 98% of energy in 4×4 low frequency coefficients, as reported in [39]. Additionally, the quantization step in image compression often zeroed the high frequency components [108]. Therefore, we have proposed to apply the pruned version and compute the 4×4 low frequency coefficients only. By doing that, we will save in the computational requirements and obtain the following proposed semi-orthogonal matrix transformation:

$$T_{4\times8} = \begin{bmatrix} 1 & 1 & 1 & 1 & 1 & 1 & 1 & 1 \\ 1 & 1 & 1 & 0 & 0 & -1 & -1 & -1 \\ 1 & 0 & 0 & -1 & -1 & 0 & 0 & 1 \\ 1 & 0 & -1 & -1 & 1 & 1 & 0 & -1 \end{bmatrix} \quad (3.24)$$

The signal flow graph (SFG) of the proposed matrix transformation $T_{4\times8}$ is depicted in Figure 3.5.

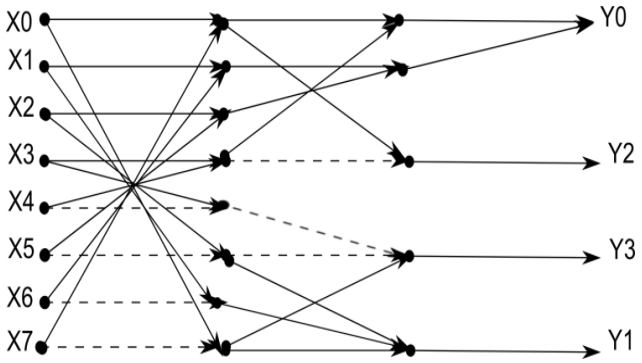

Figure 3.5. *Signal flow graph for the proposed matrix* $T_{4\times8}$. $X_i(i=0,1,\ldots7)$ *represents input data related to output data* $Y_j(j=0,1,\ldots3)$ *according to* $Y_{4\times1}=C_{4\times8}\times X_{8\times1}$ *. Dashed arrows are multiplied by -1.*

Let $X_{8\times8}$ be an 8×8 block of an image. In the proposed method we adopt L=4, thus, the proposed forward and inverse Pruned DCT approximations are given respectively by:

$$Y_{4\times4} = C_{4\times8} \cdot X_{8\times8} \cdot C_{8\times4}^{t} = D(T_{4\times8} \cdot X_{8\times8} \cdot C_{8\times4}^{t})D \quad (3.25)$$

$$X_{8\times8} = C_{8\times4}^{t} \cdot Y_{4\times4} \cdot C_{4\times8} = T_{8\times4}^{t}(D.Y_{4\times4}.D)T_{4\times8} \quad (3.26)$$

Where superscript t indicates matrix transposition, $C_{4\times 8}$ is a semi-orthogonal matrix and D is a scaling diagonal matrix, given by:

$$D = \begin{bmatrix} \frac{1}{2\sqrt{2}} & 0 & 0 & 0 \\ 0 & \frac{1}{\sqrt{6}} & 0 & 0 \\ 0 & 0 & \frac{1}{2} & 0 \\ 0 & 0 & 0 & \frac{1}{\sqrt{6}} \end{bmatrix} \tag{3.27}$$

The matrix D can be integrated into the quantization/dequantization step as suggested in many papers in the literature [83], [85-87], and does not introduce any computational overhead in the transformation stage.

By exploiting the separability property, the proposed 2-D DCT approximation [75], forward and inverse are computed with two passes of 1-D transform using row-column method [47] described before. Figure 3.6 presents the different steps adopted for the realization of the proposed 2D approximation architecture.

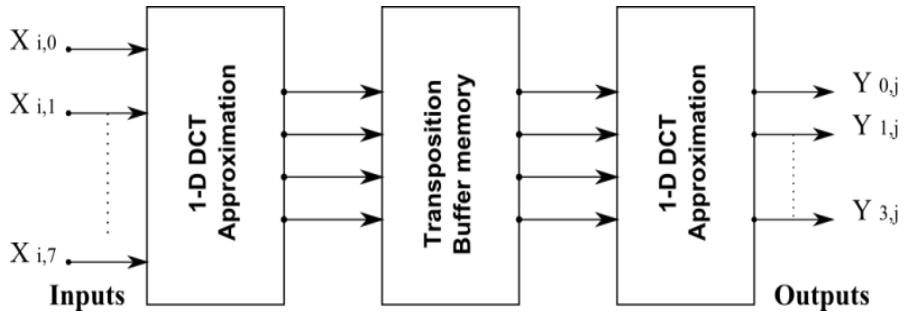

Figure.3.6. *Architecture of the proposed 2-D approximation* $X(i,j): i,j = 0,1,\ldots 7$ *represents input data.* $Y(i,j): i,j = 0,1,\ldots 3$ *represents the outputs Major Headings .*

3.6.1.2 Performance Evaluation

We investigated the proposed method in terms of image quality, processing time and energy consumption. We conducted experiments using the Atmel ATmega128L platform to measure the computation time and the resultant energy savings. We compared only pruned transformations that output L-point vector $(L<8)$ and that has been designed specifically for WSNs.

3.6.1.2.1 Results in terms of image quality:

The images shown in Figure 3.1 are compressed at 0.3 bpp by the transforms presented in [68], [66] and the proposed method [75]. Figure 3.7 shows an example of reconstructed images.

Proposed [75] (PSNR=24.16dB) [68] (PSNR=24.21dB) [66] (PSNR=22.11 dB)

Proposed [75] (PSNR=31.29dB) [68] (PSNR=30.99dB) [66] (PSNR=28.22dB)

Proposed[75] (PSNR=27.28dB) [68] (PSNR=26.92dB) [66] (PSNR=24.20dB)

Figure 3.7 *Reconstructed images at 0.3 bpp using different transformations*

Figure 3.8 shows the performance of the proposed method in terms of PSNR and MSE for the test image Lena. The transform presented in [68] leads to superior PSNR compared to the transform presented in [66]. For this reason we do not include it in the curves below.

Comparison of the curves clearly shows that the proposed transform outperforms the methods presented in [67] and [68] in terms of PSNR and MSE at a low bit rate which is the significant requirement for resource constrained WSNs. Since, only 2×2 coefficients are computed in the transform developed in [67], this scheme does not guarantee high-quality

reconstructed images. Note that, the proposed method maintains the same PSNR and MSE gain as compared to the aforementioned techniques for the whole test images.

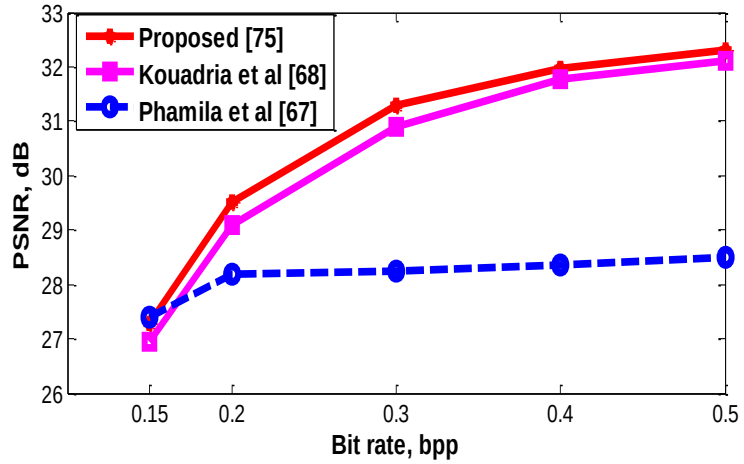

(a)

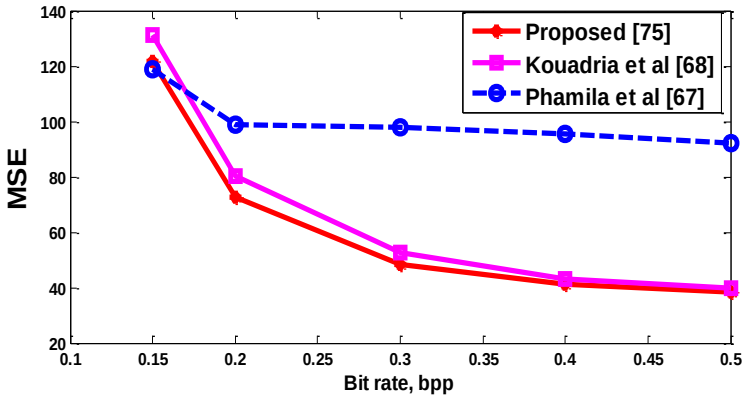

(b)

Figure 3.8. *Quality measures depending on compression ratio for different transforms.*

(a) PSNR, (b) MSE

3.6.1.2.2 Results in terms of number of operations, energy consumption and execution time

- ***Complexity assessment in terms of number of operations***

Table 3.2 summarizes the number of operations required to compute 1D transform by a different DCT approximations. Demanding only 16 additions, the proposed 1-D transform leads to 20%, 36% and 60% of arithmetic operations savings compared with the works

presented in [68], [67] and [66] respectively. Note that, for [66] and [68] the values of arithmetic complexity AC_{1-D} are provided for a pruning parameter equal to 4.

Method	Add	Shifts	Total
Lecuire et al [66]	29	11	40
Phamila et al [67]	19	6	25
Kouadria et al [68]	20	0	20
Proposed [75]	16	0	16

Table.3.2: *Arithmetic complexity* (AC_{1-D}) *of different 1-D DCT approximations.*

Table 3.2 summarizes the number of operations required to compute different 2-D DCT approximations using formulas (3.11) and (3.12).

Method	Add	Shifts	Total
Lecuire et al [66]	348	132	480
Phamila et al [67]	190	60	250
Kouadria et al [68]	240	0	240
Proposed [75]	192	0	192

Table.3.3: *Arithmetic complexity* (AC_{2-D}) *of different 2-D DCT approximations.*

The computational complexity for the proposed 2-D DCT approximation is 192. Thus, it can be seen from Table 3.3 that the proposed transform is of less complexity than the other transformations. It requires up to 60% less arithmetic operations.

- ***Complexity assessment in terms of execution time and energy consumption***

The results, in terms of computation cycles per 8 × 8 blocks for various 2-D transform are given in Table 3.4. From this Table, it is clear that the proposed transform requires less number of cycles compared to the other techniques. Table 3.5 shows the processing time and energy consumption obtained using different transforms. As expected, because of the substantial reduction in the number of arithmetic operations, the proposed transform is more efficient in speed and energy. On average, it managed to save 14%, 41% and 75% on both the processing time and energy consumption, compared with the methods presented in [68], [67] and [66] respectively. This would considerably increase the lifetime of the wireless sensor node.

So, results indicate that the proposed transform not only reduces the execution time and energy consumption, but also provides superior results in terms of PSNR performance compared with recent works.

Transform	**Cycles**
IJG float [65]	580106
Lecuire et al [66]	2734
Phamila et al [67]	1840
Kouadria et al [68]	1113
Proposed [75]	1036

Table.3.4: *Computation cycles per 8 × 8 block obtained by different 2-D transforms on the ATmega128L platform*

Transform	**Execution time (ms)**	Energy consumption (µJ)
IJG float [65]	72.51	1595.22
Lecuire et al [66]	0.37	8.53
Phamila et al [67]	0.23	5.06
Kouadria et al [68]	0.15	3.47
Proposed [75]	0.13	2.99

Table.3.5: *Execution time and energy consumption per 8 × 8 block obtained by different transforms on the ATmega128L platform.*

The proposed DCT approximation has a low complexity which combines the rounded DCT with a pruned approach. The proposed method requires 16 and 192 addition operations for 1D and 2D respectively. Experimental comparisons with recent works, using Atmel Atmega128L platform, show that the proposed scheme reduces the energy consumption, processing time and provide a better performance in terms of PSNR metric. This makes it quite suitable to be used in WISNs with a prospect to increase the lifetime of the sensor nodes. We believe that a hardware implementation in ASIC/FPGA will provide an even better performance, and will be considered in the future work.

3.6.2 Second proposed 8 by 8 DCT approximation

3.6.2.1 Mathematical concept

The methods presented in [83] and [85] are simple and prominent. They consist in applying an integer function to the standard DCT matrix in order to obtain its entries in the set $\{-1,0,+1\}$. Our proposed transform is obtained in a similar way. First, the standard 8×8 DCT matrix ($DCT_{8\times8}$) is scaled by 3, then its elements are fed into a *round* function. This results in the matrix $T_{8\times8} = round\{3 * DCT_{8\times8}\}$ that is given as follows:

$$T_{8\times8} = \begin{bmatrix} 1 & 1 & 1 & 1 & 1 & 1 & 1 & 1 \\ 1 & 1 & 1 & 0 & 0 & -1 & -1 & -1 \\ 1 & 1 & -1 & -1 & -1 & -1 & 1 & 1 \\ 1 & 0 & -1 & -1 & 1 & 1 & 0 & -1 \\ 1 & -1 & -1 & 0 & 1 & 1 & -1 & 1 \\ 1 & -1 & 0 & 1 & -1 & 0 & 1 & -1 \\ 1 & -1 & 1 & -1 & -1 & 1 & -1 & 1 \\ 0 & -1 & 1 & -1 & 1 & -1 & 1 & 0 \end{bmatrix} \quad (3.28)$$

Where the function $T_{8\times8} = round\{\bullet\}$ rounds the elements of the matrix to the nearest integer, and is defined as follows:

$$round\{x\} = sign(x).floor(|x| + \tfrac{1}{2}) \quad (3.29)$$

The matrix $T_{8\times8}$ is not orthogonal. It can be orthogonalized according to [109] using the diagonal adjustment matrix $D_{8\times8} = \sqrt{(T_{8\times8}.T_{8\times8}^{t})^{-1}}$ This procedure of orthogonalization leads to the following proposed DCT approximation matrix $C_{8\times8} = D_{8\times8} \cdot T_{8\times8}$ It can be verified that this transformation matrix is orthogonal (i.e. $C_{8\times8}^{-1} = C_{8\times8}^{t}$), where t denotes the matrix transpose operation.

A fast algorithm for the matrix $T_{8\times8}$ was derived and is depicted in Figure 3.9. According to this proposed algorithm the computation of the proposed DCT approximation requires 24 and 384 additions for the 1-D and the 2-D versions respectively.

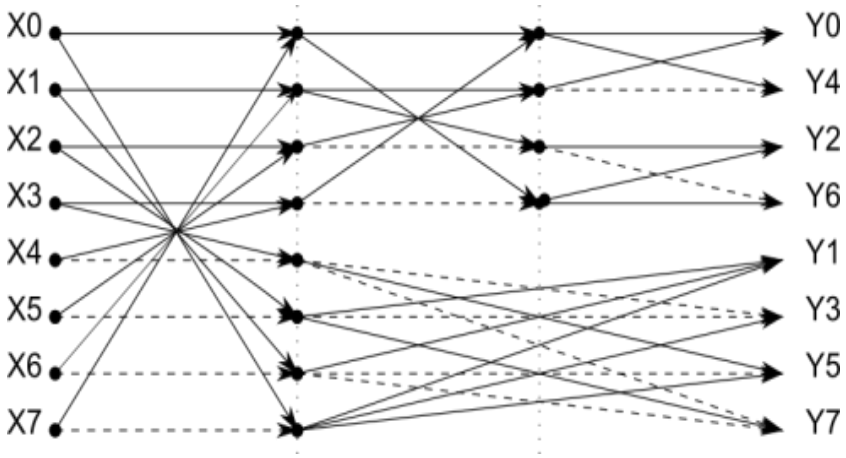

Figure 3.9 Signal flow graph for the proposed matrix $T_{8\times8}$. Xi (i = 0,1,…7) represents input data relates to output data Yj (j = 0, 1…7) according to $Y_{8\times1} = T_{8\times8} \cdot X_{8\times1}$. Dashed arrows are multiplications by -1

To further reduce computational complexity of the proposed DCT approximation, we used the 2-D pruning approach described before (section 3.4.2).

3.6.2.2 Performance Evaluation

3.6.2.2.1 Results in terms of image quality

To evaluate the performance of the proposed transform in image compression, we used it as part of the JPEG chain. This JPEG chain includes standard quantization table and Huffman encoder that are given in the JPEG standard [79]. For this purpose, we considered a set of 512×512 8-bit standard grayscale images taken from [80].

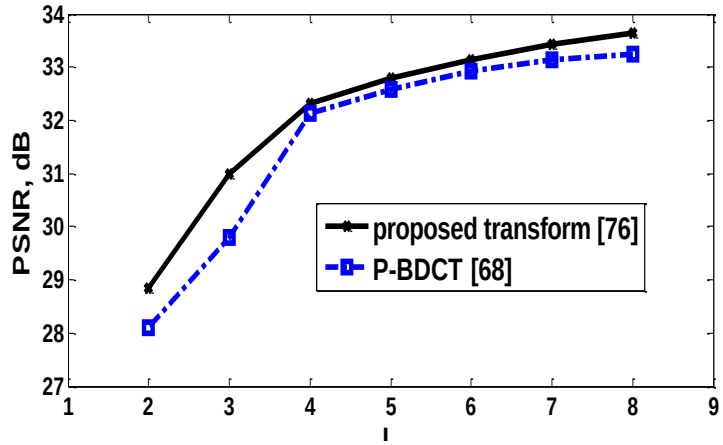

(a)

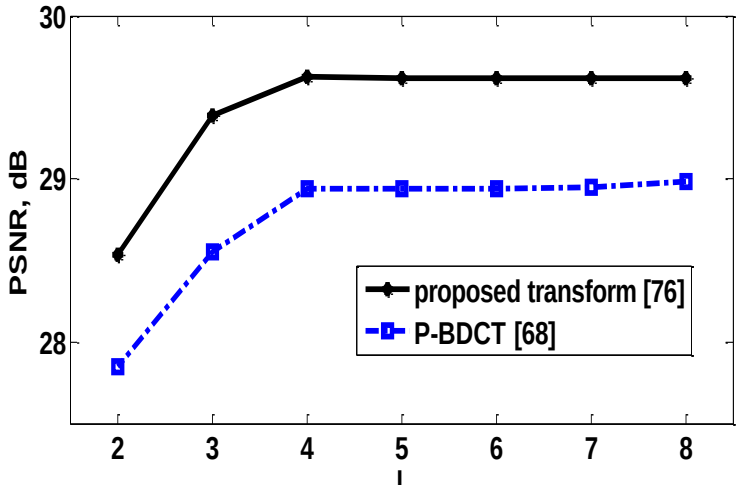

(b)

Figure. 3.10 *PSNR against L parameter for P-BDCT [68] and proposed transform[76]. Results are given for the image Lena. Fig.2a and Fig.2b correspond to bit rate of 0.5 bpp and 0.2 bpp respectively*

Table 3.6 provides the resulting PSNR for the proposed transform and P-BDCT [68] for the same complexity (i.e. L = 8) and bitrate = 0.5 bpp. It is clear from this table that the proposed transform leads to superior performances in terms of image quality. An average of 0.3 dB in PSNR gain was obtained.

Method	**Barbara**	**Lena**	**Baboon**	**Boat**	**Peppers**
Proposed [76]	27,01	33,64	23,46	29,62	32,18
P-BDCT [68]	26,71	33,25	23,24	29,35	31,82

Table.3.6: *PSNR obtained by the proposed transform [76] and P-BDCT [68]. Results are given for the same complexity (L= 8) and bit rate = 0.5 bpp.*

Figure 3.10a and Figure 3.10b show the PSNR against L using the two transforms at a bit rate of 0.5 and 0.2 bpp respectively. It can be easily seen that the proposed transform outperforms P-BDCT [68] in terms of PSNR whatever the values of L and bitrate are. The average PSNR gain is about 0.56 dB. Note that, for a large set of test images, the method maintains the same performance and doesn't depend on the image type.

3.6.2.2.2 Results in terms of number of operations, execution time and energy consumption

- ***Complexity assessment in terms of number of operations***

Table.3.7 summarises the number of additions required to compute an 8×8 block using the proposed 2-D transform compared to P-BDCT [68]. It can be seen from Table 3.6 that the proposed 8x8 DCT approximation is of less complexity than the transform P-BDCT [68]. It requires about 9 % less arithmetic operations. Therefore, the proposed transform is expected to perform better in terms of energy consumption at the WISN nodes.

L	P-BDCT [68]	Proposed[76]
L = 8	384	384
L = 7	345	330
L = 6	308	294
L = 5	273	247
L = 4	240	216
L = 3	187	165
L = 2	140	120

Table.3.7: *Computation complexity analysis. results are given for 2-D*

- ***Complexity assessment in terms of execution time and energy consumption***

The main concern in resource constrained WISNs is to reduce energy consumption as much as possible. To assess the energy efficiency of the proposed 8×8 DCT approximation in sensor nodes, we perform an experiment similar to that in [68] and [66]. For this purpose, we adopt the well-known Atmel Atmega128L platform. Results, in terms of computation cycles, execution time and energy consumption per 8×8 blocks for the proposed transform and for P-BDCT [68] are given in Table 3.8. From this table, it is clear that the proposed transform requires less cycles than the transform P-BDCT [68]. As expected, because of the reduction in the number of arithmetic operations, the proposed transform is more efficient in energy. On average, it managed to save about 10% on both the execution time and energy consumption as compared to the work in [68]. This will certainly result in a tangible increase in the lifetime of the WISN nodes.

	P-BDCT [68]			**Proposed [76]**		
	Cycles	**Time (µs)**	**Energy (µj)**	**Cycles**	**Time (µs)**	**Energy (µj)**
L =8	1850	250	5,77	1843	249	5,73
L = 7	1666	225	5,18	1584	214	4,92
L = 6	1450	196	4,52	1381	187	4,3
L = 5	1274	172	3,97	1136	154	3,54
L =4	1113	150	3,47	993	134	3,08
L = 3	890	120	2,78	775	105	2,41
L = 2	700	94	2,18	552	74	1,7

Table.3.8: *Computation cycles, execution time and energy consumption obtained by the proposed transform [76] and P-BDCT [68] on the Atmega128 L platform*

The proposed transform not only reduces the execution time and energy consumption, but also provides superior results in terms of PSNR. The obtained experimental results show that the proposed scheme reduces the energy consumption, when compared to P-BDCT, while at the same time provides a better performance in terms of PSNR metric.

3.6.3 Proposed Pruned DTT approximation

3.6.3.1 Mathematical concept

The discrete Tchebichef transform (DTT) is a novel polynomial-based orthogonal transform. It exhibits interesting properties, such as high energy compaction, optimal decorrelation and direct orthogonality, and hence is expected to produce good transform coding results. Advances in the areas of image and video coding have generated a growing interest in discrete transforms. The demand for high quality with a limited use of computational resources and improved cost benefits has led to experimentation with novel transform coding methods. In this part, we will use an approximation of the Discrete Tchebichef transform in JPEG baseline for image compression.

The discrete Tchebichef transform (DTT) is an orthogonal transformation drifted from the discrete Tchebichef polynomials (DTP) [72].

1D Forward and inverse transforms for a block of 8×8 are given by: $Y_{8\times8} = C_{8\times8} \cdot X_{8\times8}$ and $X_{8\times8} = C^{-1}_{8\times8}.X_{8x8} = C^{t}_{8X8}.X_{8x8}$

Where $X_{8\times8}$ and $Y_{8\times8}$ are the input and transformed signals, respectively. $C_{8\times8}$ can be described by the following equation: $C_{8\times8} = D_{8\times8} \cdot T_{8\times8}$, where $D_{8\times8}$ is a diagonal matrix and $T_{8\times8}$ is an integer matrix. From [74] $T_{8\times8}$ is given by:

$$T_{8\times8} = \begin{bmatrix} 1 & 1 & 1 & 1 & 1 & 1 & 1 & 1 \\ -7 & -5 & -3 & -1 & 1 & 3 & 5 & 7 \\ 7 & 1 & -3 & -5 & -5 & -3 & 1 & 7 \\ -7 & 5 & 7 & 3 & -3 & -7 & -5 & 7 \\ 7 & -13 & -3 & 9 & 9 & -3 & -13 & 7 \\ -7 & 23 & -17 & -15 & 15 & 17 & -23 & 7 \\ 1 & -5 & 9 & -5 & -5 & 9 & -5 & 1 \\ -1 & 7 & -21 & 35 & -35 & 21 & -7 & 1 \end{bmatrix} \tag{3.30}$$

The diagonal matrix $D_{8\times8}$ is given by equation (3.21):

$$D_{8\times8} = \frac{1}{2}.diag\left(\frac{1}{\sqrt{2}}, \frac{1}{\sqrt{42}}, \frac{1}{\sqrt{42}}, \frac{1}{\sqrt{66}}, \frac{1}{\sqrt{154}}, \frac{1}{\sqrt{546}}, \frac{1}{\sqrt{66}}, \frac{1}{\sqrt{858}}\right) \tag{3.31}$$

The matrix $D_{8\times8}$ can be merged into the quantization step as suggested in many works in literature [73], [74], [110] and [85], and thus it does not introduce any computational overhead. Hence the matrix $T_{8\times8}$is the only source of computational complexity. As it is described in [74], the fast algorithm for computing the matrix $T_{8\times8}$ requires 44 additions and 29 shift operations.

- *Pruned Discrete Tchebichef Transform (P-DTT)*

The proposed method is kind of approximation that is based on pruned approach and the integer DTT presented in [74]. Our main focus is to reduce the computational complexity of the exact DTT. For that raison, we use the 2-D pruning approach introduced previously.

Since most of the block energy is compacted in the first 4×4 low frequency coefficients, in this work we adopted L=4. By doing so, the forward and inverse proposed 2D P-DTT will be as it is mentioned in formulas (3.25) and (3.26) respectively, and the diagonal matrix is given by:

$$D_{4\times4} = \begin{bmatrix} \frac{1}{\sqrt{2}} & 0 & 0 & 0 \\ 0 & \frac{1}{\sqrt{42}} & 0 & 0 \\ 0 & 0 & \frac{1}{\sqrt{42}} & 0 \\ 0 & 0 & 0 & \frac{1}{\sqrt{66}} \end{bmatrix} \quad (3.32)$$

- *Fast algorithm of the proposed P-DTT:*

Based upon [74] and the pruning approach presented in subsection A, we have deducted a fast algorithm of the proposed P-DTT. Table 3.9 presents the different steps for the calculation of this algorithm. Where X=[x_0, x_1, …, x_7] is an 8-point input vector and Y=[y_0, y_1, y_2, y_3] is a 4-point output vector

Step 1	$u_0 = x_0 + x_7$	$v_0 = x_0 - x_7$
	$u_1 = x_1 + x_6$	$v_1 = x_1 - x_6$
	$u_2 = x_2 + x_5$	$v_2 = x_2 - x_5$
	$u_3 = x_3 + x_4$	$v_3 = x_3 - x_4$
Step 2		$z_0 = v_0 + v_3$
	$k_0 = u_0 + u_2$	$z_1 = v_1 - v_2$
	$k_1 = u_1 + u_3$	$z_2 = v_1 + v_2$
Step3	$m_0 = k_0 + k_1$	
	$m_2 = 2(3u_0 - 2u_2)$	$w_0 = -(z_1 + z_0)$
Step4	$l_0 = m_0 + m_2$	
	$l_4 = w_0 - 6v_0$	$l_5 = 2(2v_3 + 3z_2)$
Step5	$y_0 = m_0$	$y_2 = l_0 - 6u_3$
	$y_1 = l_4 - 4z_2$	$y_3 = l_4 + l_5$

Table.3.9: *Fast algorithm for the proposed 1D P-DTT*

Since all the involved multiplication coefficients are integer, it can be implemented by a series of shift and addition operations. These operations are presented in Table 3.10, where the shift is designed by <<.

$m \times 2 =<< m$
$m \times 3 =<< m + m$
$m \times 4 =<<<< m$
$m \times 6 =<< (<< m + m)$

Table.3.10: *Multiplication through add and shift operations*

3.6.3.2 Performance Evaluation

3.6.3.2.1 Results in terms of image quality

This section provides a comparative analysis of the performance of our proposed method with the integer DTT in [74] and the popular Loeffler DCT algorithm presented in [50]. For this purpose we used a set of standard 512×512 8-bit gray-level images taken from [80], see Figure 3.1. We performed a JPEG like simulation that includes standard quantization table and Huffman encoder that are given in the JPEG standard [79].

As the PSNR and MSE have been proved to be less inconsistent with human eye perception, we also adopted the structural similarity index (SSIM) [80], [109]. This latter is best known for his consistent with the human visual system (HVS)

- *Loeffler DCT and integer DTT comparison:*

Figure.3.11 presents the PSNR performance of the Loeffler DCT algorithm [50] and the integer DTT [74]. In this graph; we consider the average PSNR of all tested images cited in section (3.3.1) as figure of merit. According to [85], average calculation may provide more robust results than results obtained from each particular image.

Comparison of the curves clearly shows that the DTT has almost the same performances in PSNR as the DCT in low bitrates, and it is slightly lower in high level of bitrates.

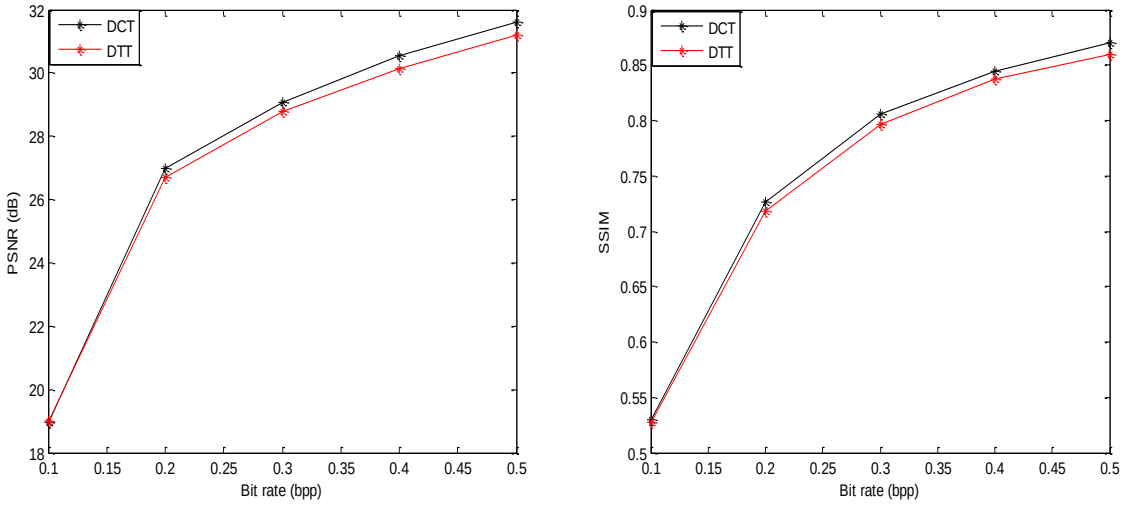

(a) (b)

Figure.3.11: *(a) Average PSNR, (b) average SSIM , for several compression ratios for: the exact DCT and the exact DTT*

- *Loeffler DCT, integer DTT and proposed P-DTT for different values of L comparison:*

PSNR and SSIM values computed from the reconstructions of tested images using: DCT, exact DTT and proposed method for different values of L are plotted in Figure. 3.12 and Figure. 3.13 respectively.

From PSNR results, it can be easily seen that the proposed method has the same performance in low bitrates that the DCT and the DTT for various input images. The proposed method tends to be slightly inferior in high bitrates that corresponds to low image compression ratios.

It is evident from the SSIM results shown in Figure 3.13 that the difference between the proposed P-DTT and the mentioned transforms get closer for the whole range of selected bitrates.

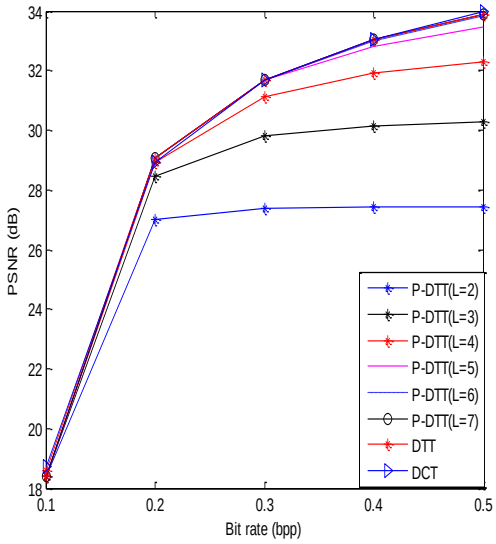

(a)

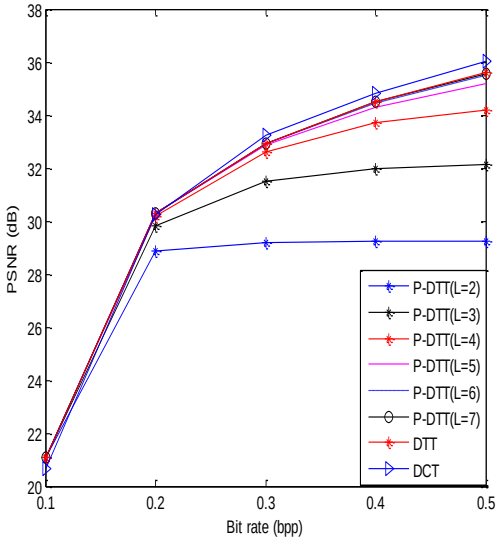

(b)

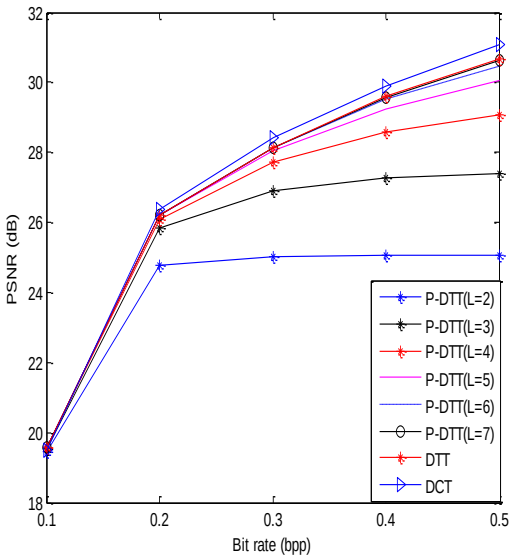

(c)

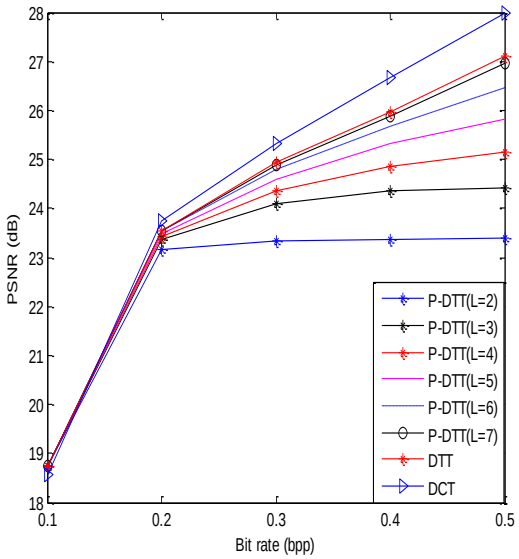

(d)

Figure. 3.12 *Rate-Distortion results of images: (a) peppers, (b) Lena,(c) boat, (d) barbara for different bit-rates*

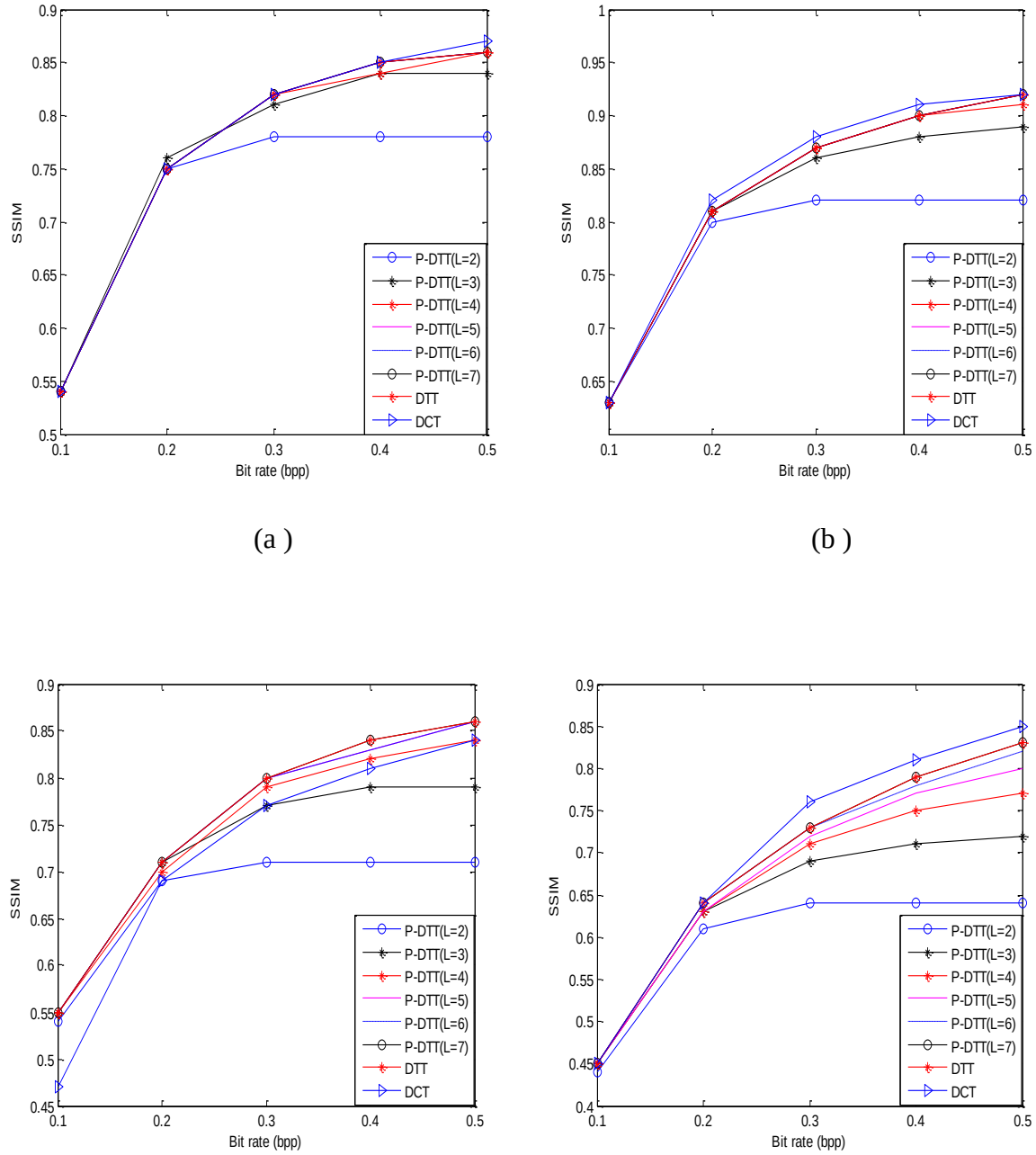

Figure. 3.13. *Structural Similarity Index (SSIM) results against bitrate For : (a) peppers, (b) Lena, ,(c) boat, (d) barbara for different bit-rates*

- *Loeffler DCT, integer DTT and proposed P-DTT for L=4 (adopted) comparison:*

Multimedia contents require extensive bandwidth and energy for transmission. Due to the limited available bandwidth and sensor power an image captured by a WSN node typically needs to be highly compressed before transmission. The appropriate bpp range for

WMSNs depends on the application in which the WMSN is involved. But, generally, WSNs require high compression ratio (small bpp < 0.5 bpp). Consider that issue; we measure the compression efficiency, at a range of [0-0.5] bpp, using the PSNR and the structural similarity index (SSIM) as figure of merits. Figure.3.14 presents the rate-distortion (R-D) curves of aforementioned transforms. The average PSNR and SSIM values (averaged over all test images) of the reconstructed images are given in Figure.3.14 (a) and (b), respectively. Average calculation may provide more robust results than results obtained from each particular image.

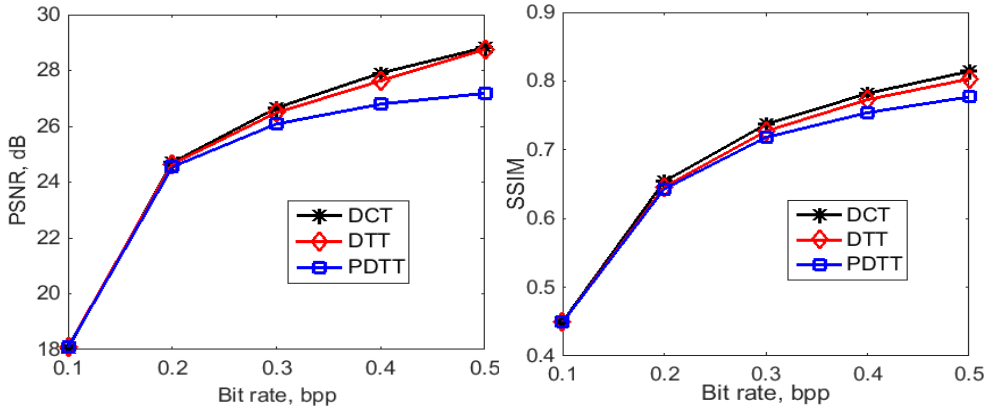

a *b*

Figure.3.14. *rate-distortion (R-D) curves of the DCT [50],DTT [74] and PDTT[77]*
(a) Average PSNR, *(b)* Average SSIM

From PSNR results in Figure.3.14 (a), it can be seen that up to 0.2 bpp the P-DTT (L=4) has the same performance than the DCT and the DTT. However, at bitrates higher than 0.2 bpp, the P-DTT performance tends to be slightly lower. Note that for perfect reconstruction of the image, the PSNR value is equal to infinity. However, in a context of lossy compression, a reconstructed image with a PSNR of 40 dB or higher, presents negligible and invisible degradations to the naked eye. If it is in the range of 25-30 dB then the image quality is typically acceptable. And this is acceptable especially in WMSNs when high quality imagery is not a relevant requirement. From SSIM results shown in Figure.3.14 (b) we observe that the difference between the three transforms (P-DTT (L=4), DTT and DCT) get closer for the whole range of selected bitrates.

- *Visual Comparison:*

PSNR=28.52dB, SSIM=0.77 (DCT [50]) PSNR=28.14dB, SSIM=0.76 (DTT[74]) PSNR=27.79dB, SSIM=0.76 (P-DTT[77])

PSNR=33.10dB, SSIM=0.88 (DCT [50]) PSNR=32.82dB, SSIM=0.87 (DTT[74]) PSNR=32.63dB, SSIM=0.87 (P-DTT[77])

PSNR=25.31dB, SSIM=0.75 (DCT [50]) PSNR=24.82dB, SSIM=0.73 (DTT[74]) PSNR=24.36dB, SSIM=0.71 (P-DTT[77])

PSNR=31.67dB, SSIM=0.82 (DCT [50]) PSNR=31.70dB, SSIM=0.82 (DTT[74]) PSNR=31.04dB, SSIM=0.82 (P-DTT[77])

Figure.3.15. Reconstructed *images using Loeffler DCT [50], exact DTT [74] and proposed P-DTT[77]. Results are given for bitrate = 0.3 bpp*

A motivating aspect of the proposed P-DTT in image compression is that the visual quality of reconstructed images is competitive compared to the other methods. To illustrate this feature, Figure 3.15 presents a visual comparison of some test images compressed at 0.3 bpp using P-DTT when L is equal to 4, Loeffler DCT [50] and integer DTT algorithms [74].

3.6.3.2.2 Results in terms of number of operations and energy consumption

- ***Results in terms of number of operations:***

Table 3.11 summarizes the number of operations required to compute the aforementioned transform for 1D and 2D.

	Calculation complexity 1D			**Calculation complexity 2D**		
Transforms	**Add**	**Mult**	**Shift**	**Add**	**Mult**	**Shift**
DCT	28	11	0	448	176	0
DTT	44	0	29	704	0	464
P-DTT L=7	38	0	24	608	0	384
P-DTT L=6	35	0	21	560	0	336
P-DTT L=5	30	0	17	480	0	272
P-DTT L=4	25	0	14	400	0	224
P-DTT L=3	22	0	11	352	0	176
P-DTT L=2	17	0	5	272	0	80

Table.3.11: *Arithmetic complexity in terms of number of operations for 1D and 2D*

Note that the Loeffler algorithm [50] reach the theoretical limit of the complexity of the exact 8-point DCT and DTT [74] is the only fast algorithm archived in literature for computing the exact 8-point DTT.

From this table, it is obviously shown that the proposed transform requires lesser complexity than the other transforms. When L is equal to 4 which we have adopted in our proposed method in [77], it requires 41 % and 52 % less additions and shift operations, respectively compared with the integer DTT [74]. Furthermore, it does not involve any multiplications, which are computationally intensive, as this is needed for Loeffler algorithm [50]. Therefore, the proposed transform yields to a considerable energy saving, thing that is suitable for embedded systems and resource constrained WSNs.

- ***Results in terms of energy consumption***

Table 3.12 represents a comparison between the energy consumption of the DTT and P-DTT when L=4, we adopted the parameters which refer to the characteristics of Mica2 platform. Mica2 platform is a well-known sensor node which contains a low-power microcontroller namely Atmel Atmeg128. As expected from the complexity analysis, we notice from the table 3.12 that the P-DTT gives better results in terms of energy efficiency. It saves about 58% of energy compared to DTT**.** These savings are for one still image and when the application requires videos, which demand several images per second, the energy reduction will be considerable. Hence, the lifetime of the battery-powered sensor node will be highly prolonged.

	Energy for 8**x**8 blocs $E_{8\times8}$(L)(**µJ**)	Energy for 512x512 Image $E_{512\times512}$(L)(**mJ**)
DTT	3,85	15,77
P-DTT L=4	1,58	6,47

Table.3.12: *Comparison between the energy consumption of DTT and P-DTT L=4*

The P-DTT computes only the upper 16 coefficients, whereas the DCT and the DTT compute the entire 64 coefficients, which require more data to be stored and processed in the working memory (RAM). Therefore, it is evident that the P-DTT requires much less memory than the other transforms. Moreover**,** we should note that this reduction propagates across the quantization and the encoding steps.

3.7 Conclusion:

In this chapter, we have proposed two low complexity DCTs approximations which have a good tradeof quality /complexity. The first proposed DCT approximation combines the rounded DCT with a pruned approach. The proposed method requires 16 and 192 addition operations for 1D and 2D respectively. Experimental comparisons with recent works, using Atmel Atmega128L platform, show that the proposed scheme reduces the energy consumption, processing time and provide a better performance in terms of PSNR metric. The second proposed DCT approximation is scaled and rounded version of the exact DCT matrix. The obtained experimental results show that the proposed scheme reduces the energy

consumption, when compared to P-BDCT, while at the same time provides a better performance in terms of PSNR metric. These results make them quite suitable to be used in WISNs with a prospect to increase the lifetime of sensor nodes.

In the other hand, we have proposed a pruned version of DTT (P-DTT) transform which requires 41 % and 52 % less additions and shift operations respectively, when compared with Loeffler DCT and the exact DTT. Moreover, the P-DTT shows competitive performance in image compression in terms of PSNR and SSIM metrics. These features make it able to be an alternative transform of DCT and it could be used in resource-limited wireless image sensor network and other digital signal processing applications that need the same constraints. These results make us believe that a hardware implementation in ASIC/FPGA will provide an even better performance, and will be considered in the future work.

Chapter 4

Region of interests coding in WMSNs

4.1. Introduction

WMSNs have limited resources nodes equipped with small camera, embedded CPU, and radio transceiver [65-68]. They ensure potential applications in different domains as we mentioned before in chapter one. One of the interesting applications of WMSN is habitat monitoring and video-surveillance [4;111-112] of a critical area of interest. In these applications a real-time transmission for the captured images between the camera nodes and the sink is necessary. Since the transmitted data has a huge volume, they must be compressed before transmission [75-77]. So, a low complexity image compression schemes adapted for WMSN, as presented in chapter 3, are desirable to compress image data without damaging its quality.

The compression standards such as JPEG or JPEG2000 save transmission bandwidth but they are not adapted to be applied in WMSNs. Indeed, these schemes are computational intensive which increases energy consumption [65;69]. In the previous chapter, we have adapted some of those compression techniques to the requirement of WMSN. We have relatively sacrificed the image quality to reduce the computational complexity. Nevertheless, it is more advantageous to maintain low complexity and/or low energy consumption and at the same time provide high image quality.

In certain scenarios, such as habitat monitoring and video-surveillance [111-112], the compression of certain parts of the image, which are called regions of interest (ROI), with a high quality to the detriment of the rest of the image (background) is one of the important steps in image processing and computer vision. The reason for that, the end user is only interested in some parts of the information, so, it would be interesting to apply a non-uniform processing to various regions of the image.

In this chapter, we have proposed a ROI based compression. The idea is to start by detecting the ROIs using a simple change detection algorithm and then we compress and transmit only these ROIs. The proposed scheme reduces the processing energy, transmission energy and the amount of transmitted data, while preserving à high quality of received images. It should be noted that the energy consumed by the wireless sensor nodes during transmission is often much higher than the energy consumed during processing (i.e.: compression program).

4.2. Proposed region-of-interest based image compression scheme

The major task of object detection is to locate objects in images and extract the regions containing them [113-115]. The quality of object detection is highly dependent on the effectiveness of finding the appropriate features and changes that exist on the current image. However, in habitat monitoring and surveillance applications image frames are often characterized by low motion [112]. So, in the beginning of the proposed scenario the camera node captures the first frame which is called the reference frame and stores it in the buffer memory. This frame will be compressed and transmitted to the sink.

In a normal situation, where a scalar node is used in addition (i.g. motion detector) to monitor the objects, if no object moves within the field of view (FoV) then the camera node stays inactive to preserve the energy. Otherwise, in case of a movement, the camera node, triggered by the scalar sensor, captures the current frame and feds it to a change detection processing block. Hence, we do not need to compress and transmit the full frame. A ROI is generated, compressed and transmitted by the sensor node to the corresponding sink. Sensor nodes only transmit the changed ROIs in the current frames according to the reference frame.

In our proposed scheme, Integer DTT [74], standard JPEG quantization and entropy coder (Huffman) are applied to compress each bloc of ROI. In contrast, uniform JPEG compression compresses all the 8by8 blocs within the frames without taking into consideration the ROI. Figure 4.1 shows a general diagram of the proposed ROI based image compression.

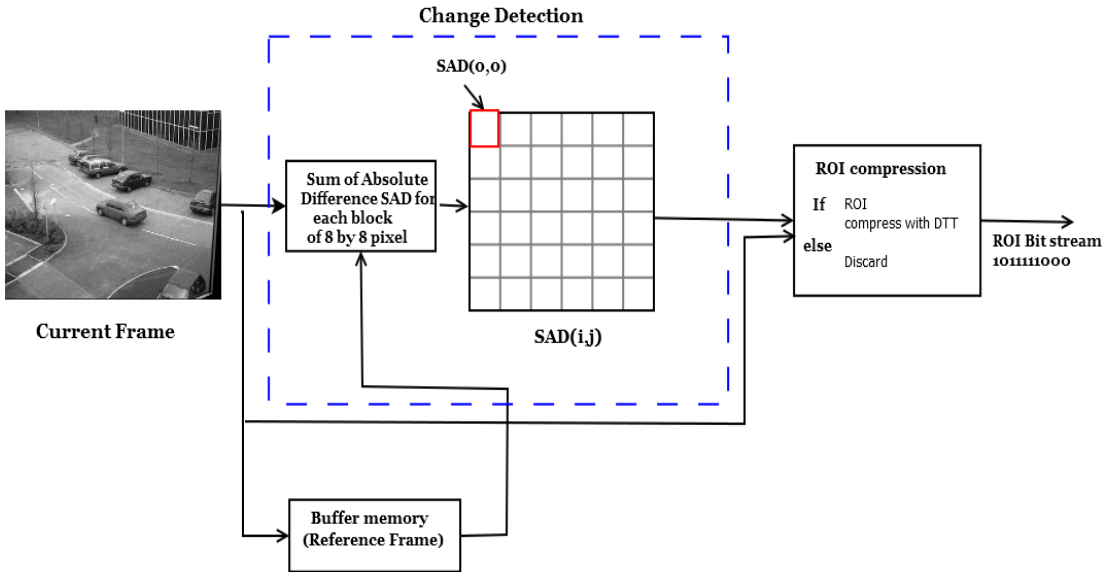

Figure.4.1. *Proposed Region-of-interest based image compression*

4.2.1 Change Detection

The main aim of habitat monitoring and video surveillance is detecting, identifying and/or tracking the object that entering the FoV. Any significant change in the scene is probably a moving object. The changed ROI are marked for further processing by the end user application, e.g., tracking or identification [116-117]. To detect the changes that occurred in a sequence of images of the same scene (static) taken at different times, a change detection algorithm is used. Its main objective is to mark the active blocks in the current frames according to the reference frame.

The proposed ROI based compression employs the sum of absolute differences (SAD) [113] as a similarity metric. The SAD algorithm measures the similarity between two images and it is calculated by taking the absolute difference between each pixel in the two images. These differences are summed to create a simple metric of similarity according to the following formula:

$$SAD_{(i,j)} = \sum_{k=0}^{7}\sum_{l=0}^{7}\left|R_{(8i+k,\ 8j+l)} - C_{(8i+k,\ 8j+l)}\right| \quad (4.1)$$

Where:

- $C_{(8i+k,\ 8j+l)}$ are the pixels of the current block
- $R_{(8i+k,\ 8j+l)}$ are the pixels of the reference block.
- (i,j) is the position of the block in the image. $1 \le i \le \frac{M}{8} - 1$ and $1 \le j \le \frac{N}{8} - 1$ which *M,N* is the image size.

SAD is a fast metric due to its simplicity compared to the other metrics. For 8by8 blocks, it takes 127 Additions and 64 absolute values. So, to simplify the analysis in our work we assume that the absolute operation is equivalent to addition operation.

In the proposed scheme, The SAD is applied inside each 8by8 block, between reference frame and current frames instead of the whole image. At each (i,j) block, the SAD is compared with a threshold TH. If the SAD result exceeds the pre-determined threshold TH, the block (i,j) is marked as changed. Thence, the marked blocks are compressed using DTT based image compression and then transmitted to the sink; however, the other blocks will be skipped. In our simulations, the value of the threshold TH is determined empirically. So, it is important to note here that the threshold is a crucial parameter and there are several works that made a detailed study on how the threshold should be chosen. If it is not chosen properly, severe quality degradation may occur. The reader can refer for instance to this papers [118-120].

At the initial stage, WMSNs only transmit one reference frame to the sink, and then they transmit only the changed parts of the frame which is different from the reference frame. To preserve a high quality of the reference frame it is compressed and transmitted as a whole. But a fast integer DTT algorithm is used to reduce the computation complexity. Computation reduction can be either achieved by using a pruned DTT or DCT approximations by calculating a subset of coefficients which contain the main energy of the image.

4.2.2. Image Reconstruction

In order to reconstruct the received image at the sink node, we superimpose it on the reference frame received earlier in the first stage. Since in the proposed approach, the portion of the image which is transmitted is marked, therefore we can easily figure out the pixel coordinates of each block. This helps in efficiently replacing the blocks in the reference frame with those of the transmitted image at the sink node. However, the transmitted data are susceptible to various effects on the channel but in our study we suppose that this data are transmitted through an ideal channel. Furthermore, the degradation will be caused by the compression only. The quality of reconstructed images is evaluated using Peak Signal to Noise Ratio (PSNR).

4. 3. Simulation and analysis

4.3.1 Change detection result:

In our simulation we test the proposed ROI-based image compression scheme on three test datasets namely: **(1)** PETS'2000[121] **(2)** Pedestrians scenario from baseline dataset [122] and **(3)** Sequence from SIPI database [123]. PETS'2000 consists of 1452 frames of 768x576 pixels in JPEG format. Pedestrians contain 2500 frames of 240×320 pixels and Sequence from SIPI database contains 10 frames of 512×512 pixels. The studied frames from each dataset are presented in Figure 4.2.

Figure 4.3 shows the reference frames from the test datasets used in the simulation. However, Figure. 4.4 shows some current frames from the test datasets.

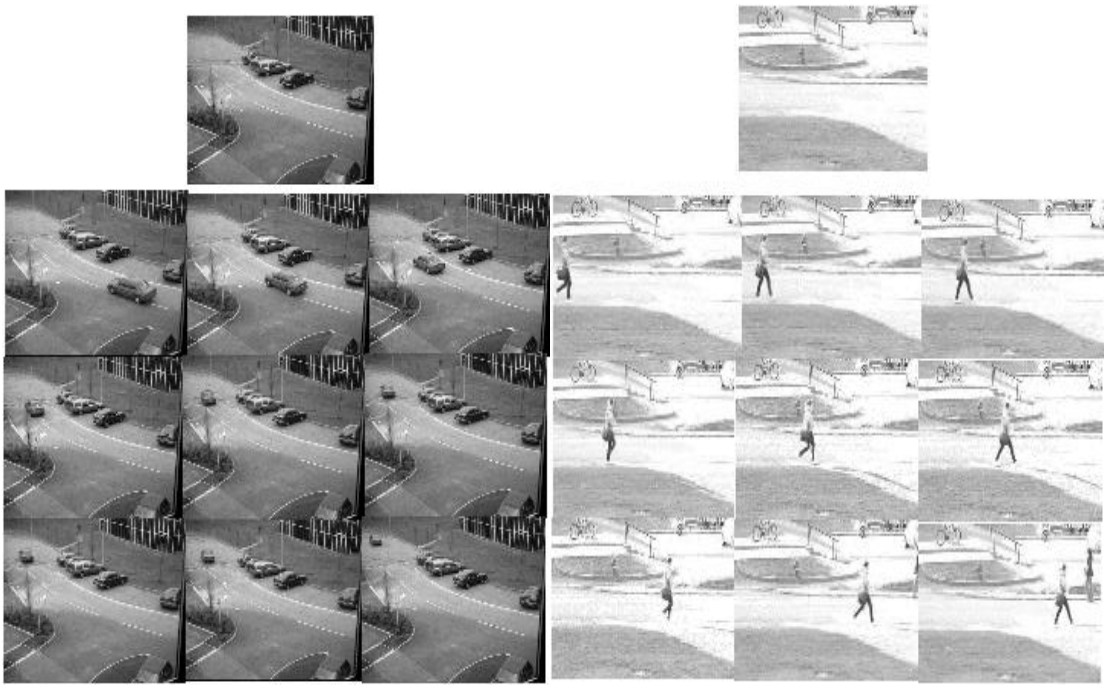

(a) (b)

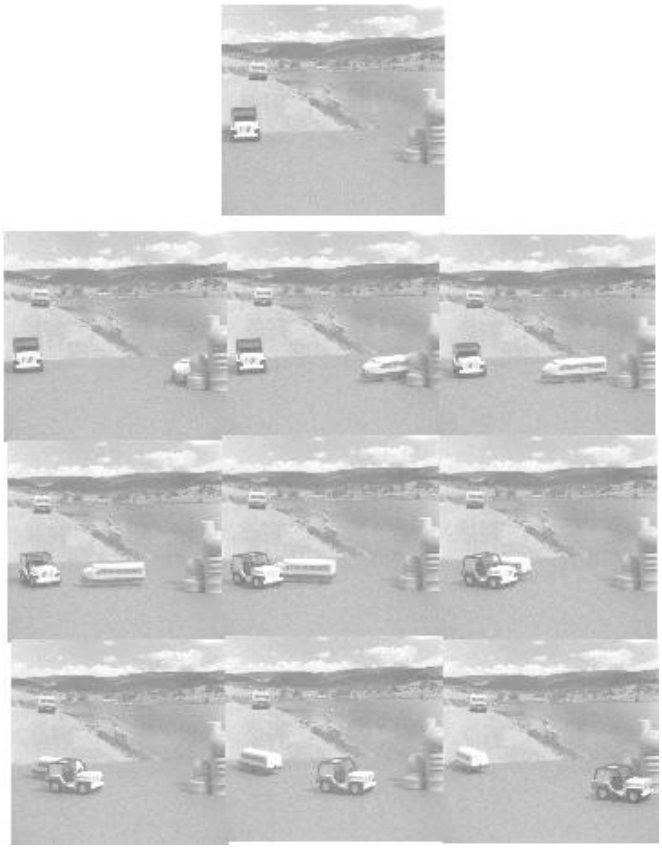

(c)

Figure.4.2: *frames from the test image Datasets used in the simulation. (a) PETS200, (c) pedestrians and (c) SIPI*

(a)

(b)

(c)

Figure.4.3: *Reference frames from the test image Datasets*.

(a)

(b)

(c)

Figure.4.4: *Current frames from the image Datasets: (a)003, (b)140 and (c) 363*

For simulation purposes, we choose ten frames from every datasets in order to test the proposed scheme. The change detection results of the selected frames from the three datasets are shown in figure 4.5. Figure.4.6 presents the results for some frames.

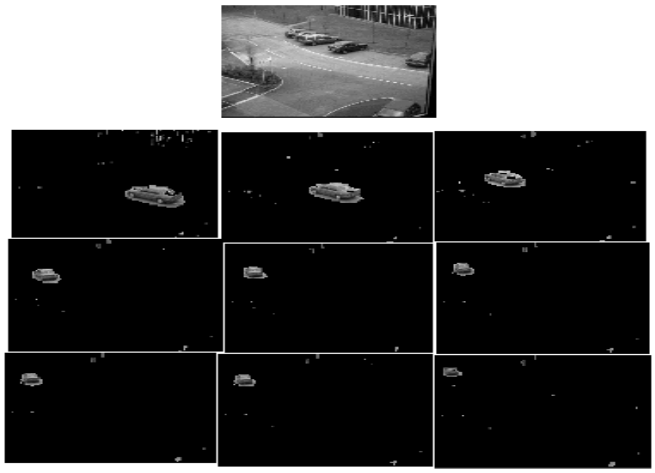

(a)

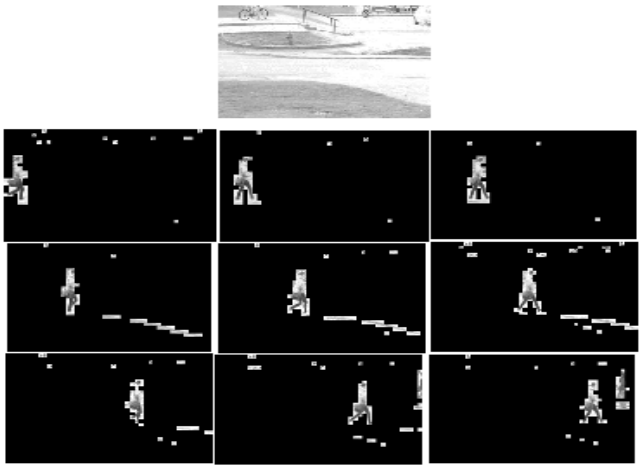

(b)

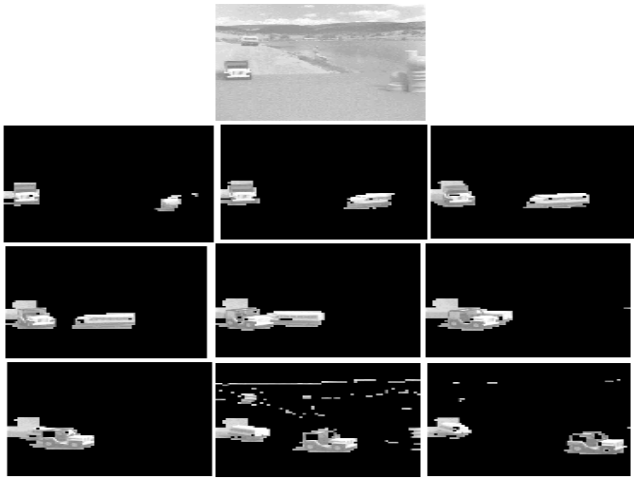

(c)

Figure.4.5. *Change detection results: from top to bottom respectively: (a) PETS2000, (b) pedestrians and (c) SIPI.*

(a)

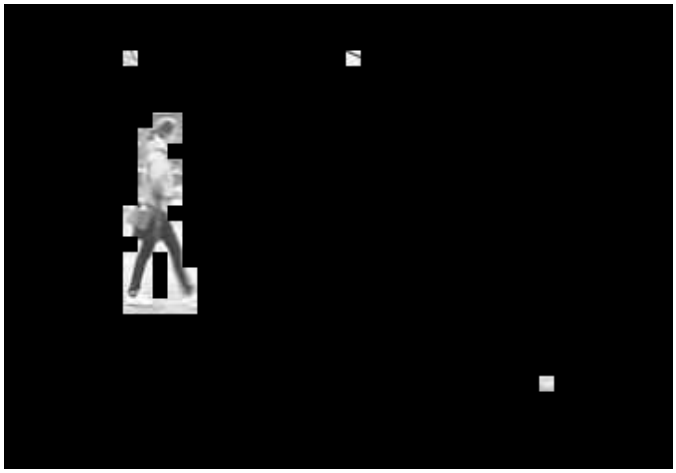

(b)

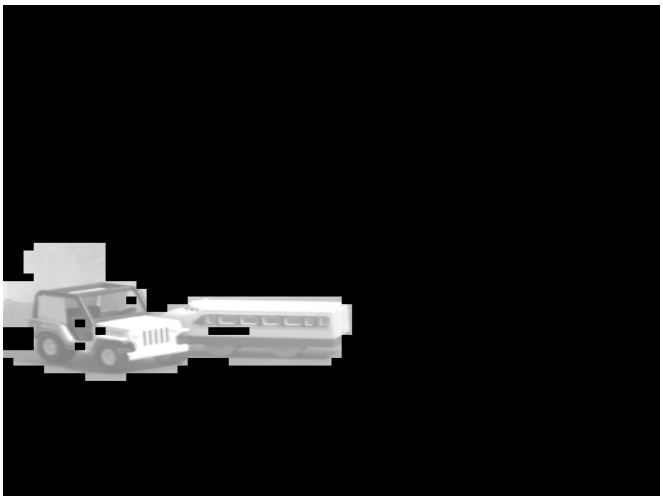

(c)

Figure.4.6. *Change detection results: from top to bottom respectively: (a) 190, (b) 341 and (c) 006*

From all above presented results, it is clear that the edges of the ROIs are very precise and we can easily distinguish the change objects in every frame. As it is clear, all the moving objects are detected by the change detection algorithm. However, there are some true negatives detected (TN: no-change blocks correctly detected) and some false negatives (FN: change blocks incorrectly detected as no-change) also known as misses in the images. We can overcome this drawback by using a sophisticated change detection algorithm (see for e.g [113]), but the main problem is its high algorithmic complexity. It is important to note that a thresholding strategy is often required to discriminate between pixels changed due to noise or to a real change.

4.3.2 Quality of the received images:

We have computed the PSNR of the received frames and we have compared it with two state-of-the-art methods namely: JPEG which uses Loeffler DCT [50] and JPEG with the BDCT [87]. We remind that the Loeffler algorithm computes the exact float DCT, and the BDCT algorithm is an intger DCT approximation. Figure.4.7 shows the PSNR of the received frames from the three datasets and figures.4.8 to 4.10 presents a visual comparison of the received frames 190, 341 and 006 from PETS2000, pedastrians and SIP datasets respectively.

From the PSNR curves presented in Figure.4.7, we see that the proposed method presents the same PSNR characteristics than JPEG compression for the PETS2000 and SIPI datasets. The average PSNR is higher than 40 dB which illustrates the high compression efficiency of the proposed method. Also, when it is applied to the pedastrians datasets the proposed method is almost in the neighbor of 40 dB and the compression efficiency stays the same.

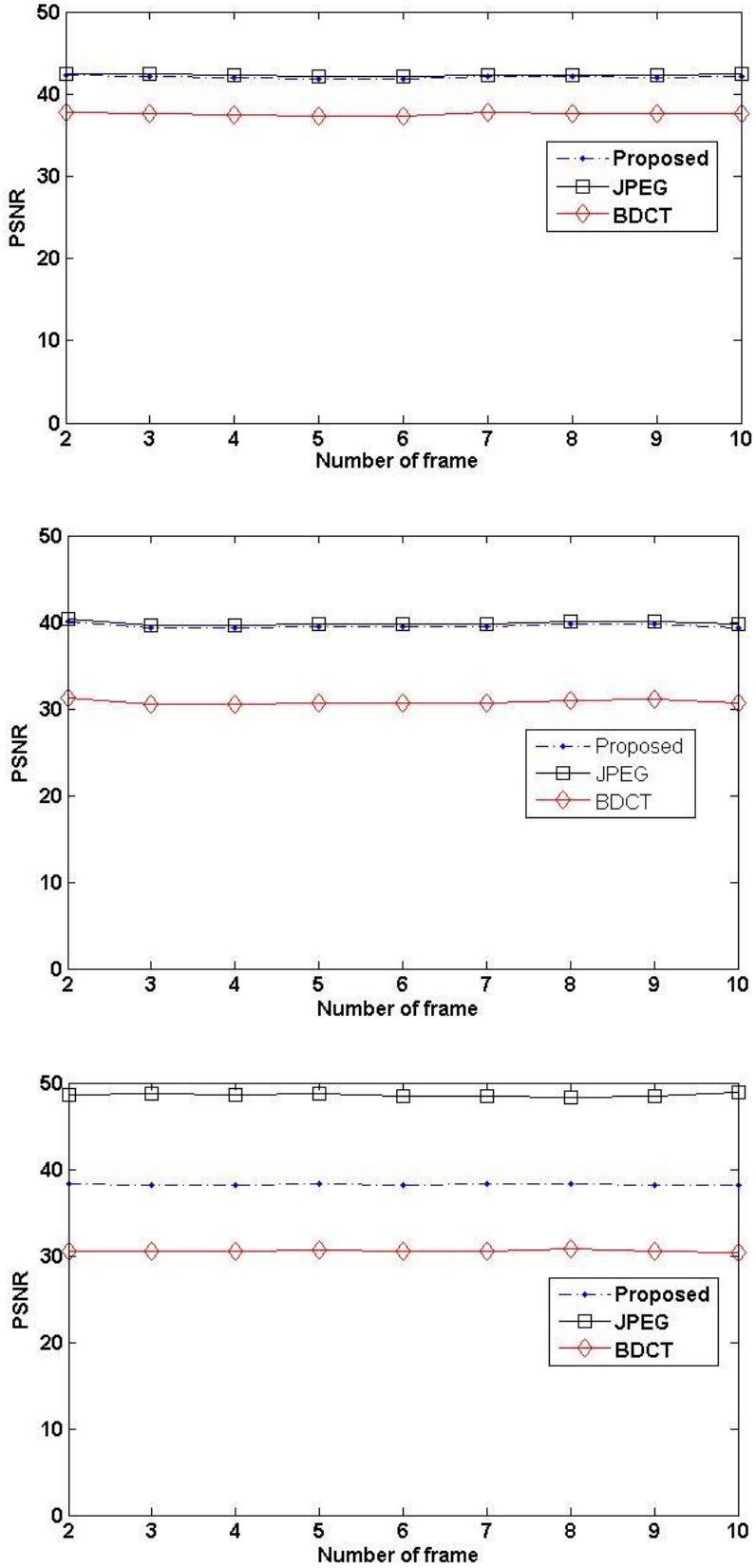

(c)

Figure.4.7. *PSNR of the received frames: from top to bottom (a) SIPI, (b) PETS200 and (c) pedestrians*

(a) BDCT=30.61 dB

(b) JPEG=39.74dB

(c) Proposed=39.44 dB

Figure.4.8. *PSNR of the received frame 190 from PETS2000. From top to bottom (a) BDCT, (b)JPEG and (c) Proposed*

(a) BDCT= 30.55 dB

(b) JPEG=48.58 dB

(c) Proposed=38.22dB

Figure.4.9. *PSNR of the received frame 341 from pedastrians. From top to bottom (a)BDCT, (b)JPEG and (c) Proposed*

(a) BDCT=37.29dB

(b) JPEG=42.07dB

(c) Proposed=41.76 dB

Figure.4.10. *PSNR of the received frame 006 from SIPI. From top to bottom (a)BDCT, (b)JPEG and (c) Proposed*

A PSNR of 40 dB or higher is a sign of high quality and the corresponding tested images present invisible and negligible degradations using the naked eye. Figure.4.8, figure.4.9 and figure 4.10 present some reconstructed frames using the proposed method, JPEG-Loeffler and JPEG-BDCT, from these reconstructed images we can verify that there is not a visual difference between the proposed method and JPEG-Loeffler. However, the visual degradation can be clearly noticed in the frames reconstructed by JPEG-BDCT.

4.3.3 Computational Complexity:

In this subsection, we compute the computational complexity of the proposed method (change detection +image compression), expressed as a number of elementary operations, and we compare it to the complexity of JPEG-Loeffler and JPEG-BDCT. Since the transformation step takes the largest part of the computational cost in image compression [70], we assume that the complexity of each compression method is taken by the transformation and hence we neglect the complexity of the quantization and entropy coders.

Tables 4.1 to 4-3 present a comparison of the complexity for the aforementioned methods when they are applied to the image datasets PETS2000, pedastrians and SIPI. Results are given for frame 5 and 6. From, these tables, we observe that the proposed method is of much less complexity than the other methods and it requires less total number of operations compared with JPEG and BDCT methods. Furthermore, it does not involve any float multiplications, which are computationally intensive, as it is needed for JPEG algorithm. Since the proposed method compresses only a portion of the image (ROI) which is detected by the change detection algorithm, the reduction in compression complexity holds true for the whole tested frames.

Frames	6			5		
Methods	Shift	Mult	ADD	Shift	Mult	ADD
Proposed	38512	0	1392448	51504	0	1412160
JPEG	0	1216512	3096576	0	1216512	3096576
BDCT	0	0	2654208	0	0	2654208

Table.4.1: *Number of operations of different methods for PETS2000*

Frames	6			5		
Methods	Shift	Mult	ADD	Shift	Mult	ADD
Proposed	32016	0	309126	27376	0	302086
JPEG	0	237600	604800	0	237600	604800
BDCT	0	0	514800	0	0	518400

Table. 4.2: *Number of operations of different methods for pedastrians*

Frames	6			5		
Methods	Shift	Mult	ADD	Shift	Mult	ADD
Proposed	164256	0	1039744	159516	0	1032704
JPEG	0	720896	1835008	0	720896	1835008
BDCT	0	0	1572864	0	0	1572864

Table4.3: *Number of operations of different methods for SIPI*

4.3.4 Energy consumption:

We can categorize the energy consumption in a typical WSN into two groups: (i) energy consumption due to processing E_{Proc} and (ii) energy consumption due to communication E_{COM}. For the computation of the energy consumption, we have used the characteristics of Mica2 sensor node and for the communication energy consumption we adopt the model presented in [124]. So the energy consumption for transmitting one bit of data at the maximum power level is E_{t1b} = 2.358 µj/bit. Hence the total energy for transmitting NB bits is given by:

$$E_{TX} = NB \times E_{t1b} \tag{4.2}$$

Communication energy is presented in tables 4.4 to 4.6.

Frame	2	3	4	5	6	7	8	9	10
Prop	146,63	137,46	130,22	119,14	115,98	115,48	115,10	115,21	112,74
JPEG	699,10	753,95	755,51	741,57	736,79	731,43	710,84	707,36	738,23
BDCT	586,14	630,28	629,34	614,77	612,04	608,60	592,56	590,14	612,15

Table.4.4: *Comparison of communication energy for PETS2000. Results are given in mJ and for Mica2 mote [124]equipped with CC1000*

Frame	2	3	4	5	6	7	8	9	10
Prop	32,71	31,46	31,05	33,19	35,65	38,21	31,85	34,81	36,11
JPEG	161,67	161,39	161,80	161,55	164,69	164,36	162,76	163,97	165,82
BDCT	153,30	153,46	153,89	153,79	156,73	156,20	154,01	156,04	157,52

Table.4.5: *Comparison of communication energy for pedastrians datasets. Results are given in mJ and for Mica2 mote [124] equipped with CC1000*

Frame	2	3	4	5	6	7	8	9	10
Prop	79,04	85,93	91,33	94,39	95,58	87,49	86,76	111,61	91,96
JPEG	199,05	206,58	210,85	213,79	214,18	205,48	205,61	209,30	205,54
BDCT	180,57	187,46	191,38	193,45	192,75	184,25	185,01	187,10	183,70

Table.4.6: *Comparison of communication energy for SIPI datasets. Results are given in mJ and for Mica2 mote [124] equipped with CC1000*

We observe from the tables above that the communication energy of the proposed method is lower as compared with JPEG and BDCT. Tables 4.7 to 4.9 present the amount of transmitted data using the aforementioned methods. From the obtained results, it is clear that the amount of transmitted data is low using the proposed method, this fact leads to communication energy savings which is in our case about 56% and 50 % compared to JPEG and BDCT, respectively.

Frame	2	3	4	5	6	7	8	9	10
Proposed	7,05	6,61	6,26	5,73	5,58	5,55	5,54	5,54	5,42
JPEG	33,62	36,26	36,34	35,67	35,44	35,18	34,19	34,02	35,51
BDCT	28,19	30,31	30,27	29,57	29,44	29,27	28,50	28,38	29,44

Table.4.7: *Amount of transmitted data for PETS2000 datasets. Results are given in* ko.

Frame	2	3	4	5	6	7	8	9	10
Proposed	1,57	1,51	1,49	1,60	1,71	1,84	1,53	1,67	1,74
JPEG	7,78	7,76	7,78	7,77	7,92	7,91	7,83	7,89	7,98
BDCT	7,37	7,38	7,40	7,40	7,54	7,51	7,41	7,51	7,58

Table.4.8: *Amount of transmitted data for pedestrians datasets. Results are given in* ko.

Frame	2	3	4	5	6	7	8	9	10
Proposed	3,80	4,13	4,39	4,54	4,60	4,21	4,17	5,37	4,42
JPEG	9,57	9,94	10,14	10,28	10,30	9,88	9,89	10,07	9,89
BDCT	8,68	9,02	9,20	9,30	9,27	8,86	8,90	9,00	8,84

Table.4.9: *Amount of transmitted data for SIPI datasets. Results are given in* ko.

Energy consumption for processing is comprised of two main components:

1) Change detection energy consumption (for the proposed only) E_{CD}.
2) Image compression energy consumption E_{COMP}.

Therefore, processing energy consumption can be expressed as sum:

$$E_{Proc}=E_{CD} + E_{COMP} \tag{4.3}$$

As we mentioned before, the change detection block requires 129 additions and 64 abs operations per 8×8 block and its total energy requirement depend on the image size. Hence the energy consumption of the change detection algorithm is obtained as follows:

$$E_{CD} = (129\varepsilon_{Add} + 64\varepsilon_{ABS})(M \times N)/64 \tag{4.4}$$

Where ε_{Add} and ε_{ABS} are the energy of the addition and Absolute operations (per byte) in the CPU, respectively. $(M \times N)/64$ is the number of 8×8 blocks in the image of size $M \times N$.To compute the compression energy, which is directly proportional to the computation complexity, we use the model developed in chapter 3 in equation (3.16).

To determine the processing energy consumption of a WSN node for a given image of size $\times N$, we use the energy model presented in equation (4.3). Tables 4.10 to 4.12 show the results of processing energy consumption for the proposed method, JPEG-Loeffler and JPEG-BDCT.

Frame	2	3	4	5	6	7	8	9	10
Proposed	5,74	5,40	5,12	4,85	4,74	4,74	4,74	4,74	4,66
JPEG	22,26	22,26	22,26	22,26	22,26	22,26	22,26	22,26	22,26
BDCT	8,78	8,78	8,78	8,78	8,78	8,78	8,78	8,78	8,78

Table.4.10: *Comparison of processing energy for PETS2000 datasets. Results are given in mJ and for Mica2 mote [124].*

Frame	2	3	4	5	6	7	8	9	10
Proposed	1,05	1,05	1,04	1,09	1,13	1,16	1,05	1,09	1,11
JPEG	4,35	4,35	4,35	4,35	4,35	4,35	4,35	4,35	4,35
BDCT	1,71	1,71	1,71	1,71	1,71	1,71	1,71	1,71	1,71

Table.4.11: *Comparison of processing energy for pedestrians datasets. Results are given in mJ and for Mica2 mote [124].*

Frame	2	3	4	5	6	7	8	9	10
Proposed	3,22	3,54	3,82	3,95	3,98	3,76	3,69	4,48	3,78
JPEG	13,19	13,19	13,19	13,19	13,19	13,19	13,19	13,19	13,19
BDCT	5,20	5,20	5,20	5,20	5,20	5,20	5,20	5,20	5,20

Table.4.12: *Comparison of processing energy for SIPI datasets. Results are given in mJ and for Mica2 mote [124]*

We observe from these tables that the energy consumption of JPEG and BDCT stay constant for the used datasets, But that of the proposed method change continuously since it compresses a variable dimension of region-of-interest. Another observation is that the energy consumption of the proposed method (change detection + compression) is lower than the both transforms JPEG and BDCT. The proposed method saves about 70 % and 30 % of energy compared to JPEG and BDCT, respectively. These savings are the consequence of a change detection block which fed to the compression block a portion of the frame only. On the other hand, uniform compression such as in JPEG and BDCT compresses the whole image which leads to arise the complexity and the energy consumption. Another cause of these energy savings is that the transform employed in the proposed method is integer and does not involve any multiplication or floating operations.

According to the calibration of the camera for the test datasets, moving objects (e.g. car, people, bird…etc) are generally small in the surveillance scene. Consequently, the change detection result data is much smaller than the full frame and this yields to a considerable reduction in the in-node energy consumption (Processing and transmission). Transmitted data is obviously decreased which will optimize the use of the WSN communication channel such as bandwidth.

4.4. Conclusion

We proposed a region-of-interest low complexity image compression scheme based on change detection and DTT transform. The change detection algorithm employs the sum of absolute differences (SAD) on 8by8 blocks to mark the motion blocks within the frames. And the DTT with its fast integer algorithm is used as a first step to compress the ROI. .

Simulations on test datasets show that the change detection algorithm can detect the change regions and this will reduce the number of blocks to be compressed and transmitted significantly. The proposed scheme preserves the energy consumption of sensor nodes and also the bandwidth in the transmission channel all this with high quality reconstructed images at the sink.

Conclusion and perspectives

Conclusion

In the last decade, WSNs has attracted many industries, universities, researchers for its wide range of applications that it could be offered by this technology. However, WSNs must resist to a large amount of challenges such as: the low memory, the limited CPU and the most important of them is the limited power supply. Energy is a critical resource and it represents a major obstacle for the deployment of this type of network. So the main target for this field of research is how to manage the energy consumption to keep the sensor node working in long time.

In this thesis, we have interested on energy efficiency in WSNs with a particular attention on local images compressions, which means compression in a sensor node. For that, we have proposed some energy efficient algorithms. These algorithms are based on the JPEG standard and have rate-distortion characteristics very close to state-of-the-art algorithms in the literature. Assessments criteria take on consideration reconstructed images quality, execution time, energy consumption and the amount of transmitted data.

The transformation is the part that consumes most of the energy; our proposed compression algorithms interested particularly to reduce the complexity of this step. In this thesis, we have proposed two low complexity DCTs approximations which have a good tradeoff quality /complexity. The first proposed DCT approximation combines the rounded DCT with a pruned approach. Experimental comparisons with recent works, using Atmel Atmega128L platform, show that the proposed scheme reduces the energy consumption, processing time and provide a better performance in terms of PSNR metric. The second proposed DCT approximation is a scaled and rounded version of the standard DCT matrix with a pruned approach. The obtained experimental results show that the proposed scheme reduces the energy consumption, when compared to P-BDCT, while at the same time provides a better performance in terms of PSNR metric. Also, we have proposed a pruned version of DTT (P-DTT) that requires 41 % and 52 % less additions and shift operations respectively, when compared with Loeffler DCT and the exact DTT. Moreover, the proposed transform shows competitive performance in image compression in terms of PSNR and SSIM metrics. These features make it able to be an alternative transform of DCT and it could be used in resource-limited wireless image sensor network and other digital signal processing applications that need the same constraints.

In the last part of this research work, we have proposed a region-of-interest based image coding. We used a change detection preprocessing block to detect the blocks that have been changed in the current frame. A non-uniform compression, which uses a DTT transform, is then applied to compress only the changed blocks. This proposed method shows the superiority against state-of-the-art methods in terms of energy efficiency and presented a good image quality.

Perspectives:

The work presented in this thesis is convincing since we arrive at significant savings in terms of energy and execution times. Therefore several perspectives can be envisaged on the basis of this work. We structure them as following:

- These works can be implemented in ASIC/FPGA, in order to allow, among other things, a real-time processing.
- More reduce the arithmetic complexity by using different types of transforms. The evaluation of these transforms could always be in terms of rate distortion and also in terms of energy consumption and execution time.
- Evaluate the impact of the proposed methods on a wide wireless sensor network.
- Investigate other change detection algorithms which possesses low algorithmic complexity and good quality of detection
- Implement the proposed methods in a real wireless sensor node like Mica2, MicaZ and Telos motes and see their impact in the energy consumption and/or image quality.

References

References

[1] Alamri, Atif, et al. "A survey on sensor-cloud: architecture, applications, and approaches." *International Journal of Distributed Sensor Networks* 9.2 (2013): 917923.

[2] Fadel, Etimad, et al. "A survey on wireless sensor networks for smart grid." *Computer Communications* 71 (2015): 22-33.

[3] Valverde, Juan, et al. "Wireless sensor network for environmental monitoring: application in a coffee factory." *International Journal of Distributed Sensor Networks* (2011).

[4] Garcia-Sanchez, Antonio-Javier, Felipe Garcia-Sanchez, and Joan Garcia-Haro. "Wireless sensor network deployment for integrating video-surveillance and data-monitoring in precision agriculture over distributed crops." *Computers and Electronics in Agriculture* 75.2 (2011): 288-303.

[5] Alemdar, Hande, and Cem Ersoy. "Wireless sensor networks for healthcare: A survey." *Computer Networks* 54.15 (2010): 2688-2710.

[6] El Barachi, May, and Omar Alfandi. "The design and implementation of a wireless healthcare application for WSN-enabled IMS environments." *Consumer Communications and Networking Conference (CCNC), 2013 IEEE*. IEEE, 2013.

[7] He, Debiao, et al. "Robust anonymous authentication protocol for health-care applications using wireless medical sensor networks." *Multimedia Systems* 21.1 (2015): 49-60.

[8] Ahmad, Ishfaq, Khalil Shah, and Saif Ullah. "Military Applications using Wireless Sensor Networks: A survey." *International Journal of Engineering Science* 7039 (2016).

[9] Lee, Sang Hyuk, et al. "Wireless sensor network design for tactical military applications: Remote large-scale environments." *Military Communications Conference, 2009. MILCOM 2009. IEEE*. IEEE, 2009.

[10] Đurišić, Milica Pejanović, et al. "A survey of military applications of wireless sensor networks." *Embedded Computing (MECO), 2012 Mediterranean Conference on*. IEEE, 2012..

[11] Akyildiz, Ian F., et al. "Wireless sensor networks: a survey." *Computer networks* 38.4 (2002): 393-422.

[12] Chandrakasan, Amirtharajah, et al. "Design considerations for distributed microsensor systems." *Custom Integrated Circuits, 1999. Proceedings of the IEEE 1999*. IEEE, 1999.

[13] Shaikh, Faisal Karim, and Sherali Zeadally. "Energy harvesting in wireless sensor networks: A comprehensive review." *Renewable and Sustainable Energy Reviews* 55 (2016): 1041-1054.

[14] Hoblos, G., M. Staroswiecki, and A. Aitouche. "Optimal design of fault tolerant sensor networks." *Control Applications, 2000. Proceedings of the 2000 IEEE International Conference on*. IEEE, 2000.

[15] Nadig, D., S. S. Iyengar, and D. N. Jayasimha. "A new architecture for distributed sensor integration." *Southeastcon'93, Proceedings., IEEE*. IEEE, 1993.

[16] Srisathapornphat, Chavalit, Chaiporn Jaikaeo, and Chien-Chung Shen. "Sensor information networking architecture." *Parallel Processing, 2000. Proceedings. 2000 International Workshops on*. IEEE, 2000.

[17] Boukerche, Azzedine, et al. "Routing protocols in ad hoc networks: A survey." Computer networks 55.13 (2011).

[18] Tiwari, Vivek, et al. "Instruction level power analysis and optimization of software." *VLSI Design, 1996. Proceedings., Ninth International Conference on*. IEEE, 1996.

[19] Sinha, Amit, and Anantha P. Chandrakasan. "Jouletrack-a web based tool for software energy profiling." *Design Automation Conference, 2001. Proceedings*. IEEE, 2001.

[20] Raghunathan, Vijay, et al. "Energy-aware wireless microsensor networks." *IEEE Signal processing magazine* 19.2 (2002).

[21] IEEE Computer Society LAN MAN Standards Committee. "Wireless LAN medium access control (MAC) and physical layer (PHY) specifications." *IEEE Standard 802.11-1997* (1997).

[22] Xu, Ya, John Heidemann, and Deborah Estrin. "Geography-informed energy conservation for ad hoc routing." *Proceedings of the 7th annual international conference on Mobile computing and networking*. ACM, 2001.

[23] Wang, Andrew, et al. "Energy efficient modulation and MAC for asymmetric RF microsensor systems." *Proceedings of the 2001 international symposium on Low power electronics and design*. ACM, 2001

[24] Soua, Ridha, and Pascale Minet. "A survey on energy efficient techniques in wireless sensor networks." *Wireless and Mobile Networking Conference (WMNC), 2011 4th Joint IFIP*. IEEE, 2011.

[25] Minet, P. "Energy efficient routing." *Ad Hoc and Sensor Wireless Networks: Architectures: Algorithms and Protocols* (2009).

[26] Almalkawi, Islam T., et al. "Wireless multimedia sensor networks: current trends and future directions." *Sensors* 10.7 (2010): 6662-6717.

[27] Akyildiz, Ian F., Tommaso Melodia, and Kaushik R. Chowdhury. "Wireless multimedia sensor networks: Applications and testbeds." *Proceedings of the IEEE* 96.10 (2008): 1588-1605.

[28] Al Nuaimi, Mariam, Farag Sallabi, and Khaled Shuaib. "A survey of wireless multimedia sensor networks challenges and solutions." *Innovations in Information Technology (IIT), 2011 International Conference on*. IEEE, 2011.

[29] Garcia-Sanchez, Antonio-Javier, Felipe Garcia-Sanchez, and Joan Garcia-Haro. "Wireless sensor network deployment for integrating video-surveillance and data-monitoring in precision agriculture over distributed crops." *Computers and Electronics in Agriculture* 75.2 (2011): 288-303.

[30] Paek, Jeongyeup, et al. "Image-based environmental monitoring sensor application using an embedded wireless sensor network." *Sensors* 14.9 (2014): 15981-16002.

[31] Ang, Li-minn, et al. *Wireless Multimedia Sensor Networks on Reconfigurable Hardware: Information Reduction Techniques*. Springer Science & Business Media, 2013.

[32] ZainEldin, Hanaa, Mostafa A. Elhosseini, and Hesham A. Ali. "Image compression algorithms in wireless multimedia sensor networks: A survey." *Ain Shams Engineering Journal* 6.2 (2015): 481-490.

[33] Shukla, Jaya, Manoj Alwani, and Anil Kumar Tiwari. "A survey on lossless image compression methods." *Computer Engineering and Technology (ICCET), 2010 2nd International Conference on*. Vol. 6. IEEE, 2010.

[34] Carreto-Castro, M. F., et al. "Comparison of lossless compression techniques." *Circuits and Systems, 1993., Proceedings of the 36th Midwest Symposium on*. IEEE, 1993.

[35] Lee, Dong-U., et al. "Energy-efficient image compression for resource-constrained platforms." *IEEE Transactions on Image Processing* 18.9 (2009): 2100-2113..

[36] Bhattacharyya, P., Mitra, A., & Chatterjee, A. (2014, January). Vector quantization based image compression using generalized improved fuzzy clustering. In *Control, Instrumentation, Energy and Communication (CIEC), 2014 International Conference on* (pp. 662-666). IEEE.

[37] Liu, Shuai, et al. "A fractal image encoding method based on statistical loss used in agricultural image compression." *Multimedia Tools and Applications* 75.23 (2016): 15525-15536.

[38] Kimura, Naoto, and Shahram Latifi. "A survey on data compression in wireless sensor networks." *Information Technology: Coding and Computing, 2005. ITCC 2005. International Conference on*. Vol. 2. IEEE, 2005.

[39] Thyagarajan, Kadayam S. *Still image and video compression with MATLAB*. John Wiley & Sons, 2011.

[40] Arici, Tarik, et al. "PINCO: A pipelined in-network compression scheme for data collection in wireless sensor networks." *Computer Communications and Networks, 2003. ICCCN 2003. Proceedings. The 12th International Conference on*. IEEE, 2003.

[41] Sayood, Khalid. *Introduction to data compression*. Newnes, 2012.

[42] Huffman, David A. "A method for the construction of minimum-redundancy codes." *Proceedings of the IRE* 40.9 (1952): 1098-1101.

[43] Witten, Ian H., Radford M. Neal, and John G. Cleary. "Arithmetic coding for data compression." *Communications of the ACM* 30.6 (1987): 520-540.

[44] Golomb, SW. "Run-length encodings". *IEEE Transactions on Information Theory*,12, 399-401. (1966).

[45] Ahmed, Nasir, T_ Natarajan, and Kamisetty R. Rao. "Discrete cosine transform." *IEEE transactions on Computers* 100.1 (1974): 90-93.

[46] Senapati, Ranjan Kumar. *Development of Novel Image Compression Algorithms for Portable Multimedia Applications*. Diss. 2012.

[47] Wallace, Gregory K. "The JPEG still picture compression standard." *IEEE transactions on consumer electronics* 38.1 (1992).

[48] Lohscheller, Herbert. "A subjectively adapted image communication system." *IEEE Transactions on Communications* 32.12 (1984): 1316-1322.

[49] Taylor, Clark N., Debashis Panigrahi, and Sujit Dey. "Design of an adaptive architecture for energy efficient wireless image communication." *Embedded processor design challenges*. Springer Berlin Heidelberg, 2002.

[50] Loeffler, Christoph, Adriaan Ligtenberg, and George S. Moschytz. "Practical fast 1-D DCT algorithms with 11 multiplications." *Acoustics, Speech, and Signal Processing, 1989. ICASSP-89., 1989 International Conference on*. IEEE, 1989 [51] Heyne, B., & Götze, J. (2007). A low-power and high-quality implementation of the discrete cosine transformation. *Advances in Radio Science*, *5*.

[52] Liang, Jie, and Trac D. Tran. "Fast multiplierless approximations of the DCT with the lifting scheme." *IEEE Transactions on Signal Processing* 49.12 (2001): 3032-3044.

[53] Britanak, Vladimir, Patrick Yip, and K. R. Rao. "Discrete cosine and sine transforms." *New York: Academic* (2007).

[54] Shams, Ahmed M., et al. "NEDA: A low-power high-performance DCT architecture." *IEEE transactions on signal processing* 54.3 (2006): 955-964.

[55] Sharma, Vijay K., Kamala K. Mahapatra, and Umesh C. Pati. "Non-recursive computation of 8× 8 2D DCT for high accuracy and low area." *Journal of Circuits, Systems, and Computers* 23.10 (2014): 1450143.

[56] Xanthopoulos, Thucydides. *Low power data-dependent transform video and still image coding*. Diss. Massachusetts Institute of Technology, 1999.

[57] Chiasserini, C-F., and Enrico Magli. "Energy consumption and image quality in wireless video-surveillance networks." *Personal, Indoor and Mobile Radio Communications, 2002. The 13th IEEE International Symposium on*. Vol. 5. IEEE, 2002.

[58] White, Stanley A. "Applications of distributed arithmetic to digital signal processing: A tutorial review." *IEEE ASSP Magazine* 6.3 (1989): 4-19.

[59] Mallat, Stephane G. "A theory for multiresolution signal decomposition: the wavelet representation." *IEEE transactions on pattern analysis and machine intelligence* 11.7 (1989): 674-693.

[60] Kidwai, Naimur Rahman, Ekram Khan, and Martin Reisslein. "ZM-SPECK: A Fast and Memoryless Image Coder for Multimedia Sensor Networks." *IEEE Sensors Journal* 16.8 (2016): 2575-2587.

[61] Ma, Tao, et al. "A survey of energy-efficient compression and communication techniques for multimedia in resource constrained systems." *IEEE Communications Surveys & Tutorials* 15.3 (2013): 963-972.

[62] Lecuire, Vincent, Cristian Duran-Faundez, and Nicolas Krommenacker. "Energy-efficient image transmission in sensor networks." *International Journal of Sensor Networks* 4.1-2 (2008): 37-47.

[63] Rein, Stephan, and Martin Reisslein. "Scalable line-based wavelet image coding in wireless sensor networks." *Journal of Visual Communication and Image Representation* 40 (2016): 418-431.

[64] Tausif, Mohd, et al. "FrWF-based LMBTC: Memory-efficient image coding for visual sensors." *IEEE Sensors Journal* 15.11 (2015): 6218-6228.

[65] D. U. Lee, H. Kim, M. Rahimi, D. Estrin, and J.D. Villasenor. Energy-efficient image compression for resource-constrained platforms. Image Processing, IEEE Transactions on, 18(9), (2009), 2100-2113..

[66] Lecuire, Vincent, Leila Makkaoui, and J-M. Moureaux. "Fast zonal DCT for energy conservation in wireless image sensor networks." *Electronics Letters* 48.2 (2012): 125-127.

[67] Phamila and R. Amutha, Low complexity energy efficient very low bit-rate image compression scheme for wireless sensor network, Inf. Process. Lett., 113 (2013) 672–676.

[68] Kouadria, N., et al. "Low complexity DCT for image compression in wireless visual sensor networks." *Electronics Letters* 49.24 (2013): 1531-1532.

[69] Ferrigno, Luigi, et al. "Balancing computational and transmission power consumption in wireless image sensor networks." *Virtual Environments, Human-Computer Interfaces and Measurement Systems, 2005. VECIMS 2005. Proceedings of the 2005 IEEE International Conference on*. IEEE, 2005.

[70] Taylor, Clark N., Debashis Panigrahi, and Sujit Dey. "Design of an adaptive architecture for energy efficient wireless image communication." *Embedded processor design challenges*. Springer Berlin Heidelberg, 2002.

[71] Li, Leida, et al. "Referenceless measure of blocking artifacts by Tchebichef kernel analysis." *IEEE Signal Processing Letters* 21.1 (2014): 122-125.

[72] Mukundan, Ramakrishnan, S. H. Ong, and Poh Aun Lee. "Image analysis by Tchebichef moments." *IEEE Transactions on image Processing* 10.9 (2001): 1357-1364.

[73] Oliveira, Paulo AM, et al. "A discrete Tchebichef transform approximation for image and video coding." *IEEE Signal Processing Letters* 22.8 (2015): 1137-1141.

[74] Prattipati, Soni, et al. "A fast 8× 8 integer Tchebichef transform and comparison with integer cosine transform for image compression." *Circuits and Systems (MWSCAS), 2013 IEEE 56th International Midwest Symposium on*. IEEE, 2013.

[75] Mechouek, K., Kouadria, N., Doghmane, N., & Kaddeche, N. Low Complexity DCT Approximation for Image Compression in Wireless Image Sensor Networks. *Journal of Circuits, Systems and Computers*, *25*(08), 1650088. (2016).

[76] Nasreddine Kouadria, Khaoula Mechouek and Noureddine Doghmane . *"Energy efficient 8 by 8 DCT approximation for image compression in wireless image sensor networks",* ICESTI'16, Annaba 2016

[77] Kouadria, N., Mechouek, K., Messadeg, D., & Doghmane, N. Pruned discrete Tchebichef transform for image coding in wireless multimedia sensor networks. *AEU-International Journal of Electronics and Communications*, *74*, 123-127. (2017).

[78] Suzuki, Taizo, and Masaaki Ikehara. "Integer DCT based on direct-lifting of DCT-IDCT for lossless-to-lossy image coding." *IEEE Transactions on Image Processing* 19.11 (2010): 2958-2965.

[79] ISO/IEC 10918-1/ITU-T Recommendation T.81, Digital compression and coding of continuous-tone still images, (accessed September 2013), http://www.jpeg.org/jpeg/.

[80] J. Kominek, Waterloo BragZone, University of Waterloo (accessed November 2014), http://links.uwaterloo.ca/Repository.html.

[81] Wang, Zhou, et al. "Image quality assessment: from error visibility to structural similarity." *IEEE transactions on image processing* 13.4 (2004): 600-612.

[82] Britanak, Vladimir, Patrick C. Yip, and Kamisetty Ramamohan Rao. *Discrete cosine and sine transforms: general properties, fast algorithms and integer approximations*. Academic Press, 2010.

[83] T. I. Haweel. A new square wave transform based on the DCT. Signal processing, 81(11), 2309-2319, (2001)

[84] T. D. Tran, The BinDCT: Fast multiplierless approximation of the DCT. Signal Processing Letters, IEEE, 7(6), 141-144, (2000)

[85] R. J. Cintra and F. M. Bayer, A DCT approximation for image compression, IEEE Signal. Process. Lett, 18, (10), 579-582, (2011)

[86] F. M. Bayer and R. J. Cintra, DCT-like transform for image compression requires 14 additions only, Electronics Letters , 48(15), 919-921, (2012)

[87] S. Bouguezel, M. O. Ahmad, and M. N. S. Swamy, Binary discrete cosine and Hartley transforms, IEEE Trans. Circuits Syst., 2013, 60,(4), pp. 989–1002.

[88] V. Britanak, New fast algorithms for the low delay MDCT computation in the MPEG-4 AAC enhanced low delay audio coding standard. Signal Processing, 105, 410-418. (2014)

[89] Atmel Atmega 128L (accessed November 2014), http:// www.atmel.com/devices /atmega128.aspx.

[90] N. Kimura and S. Latifi, A survey on data compression in wireless sensor networks. In Information Technology: Coding and Computing, 2005. ITCC 2005. International Conference on (Vol. 2, pp. 8-13). IEEE.(2005)

[91] Y. C. Wang, Data compression techniques in wireless sensor networks. Pervasive Computing, New York: Nova Science Publishers, Inc.2012

[92] M. Tausif, N. R. Kidwai, E. Khan, M. Reisslein., FrWF-Based LMBTC: Memory-Efficient Image Coding for Visual Sensors, IEEE Sensors Journal, 2015, 15, (11), pp. 6218-6228, doi: 10.1109/JSEN.2015.2456332

[93] N. R. Kidwai, E. Khan, M. Reisslein., M. ZM-SPECK: A Fast and Memory-less Image Coder for Multimedia Sensor Networks. , IEEE Sensors Journal, 2016, 16, (8), pp. 2575 - 2587, doi: 10.1109/JSEN.2016.2519600

[94] A. Chefi, A. Soudani, and G. Sicard, "Hardware compression scheme based on low complexity arithmetic encoding for low power image transmission over WSNs," AEU-Int. Journal of Electronics and Communications, vol. 68, no. 3, pp. 193-200, March 2014

[95] Nasri, M., Helali, A., Sghaier, H., & Maaref, H. (2015). Images compression techniques for wireless sensor network applications. International Journal of Speech Technology, 18(2), 205-216.

[96] Wang, Z. (1991). Pruning the fast discrete cosine transform. *IEEE Transactions on Communications*, *39*(5), 640-643.

[97] Skodras, A. N. (1994). Fast discrete cosine transform pruning. *Signal Processing, IEEE Transactions on*, *42*(7), 1833-1837.

[98] W. H. Chen, CH Smith, and S. C. Fralick, (1974). A fast computational algorithm for the discrete cosine transforms. Communications, IEEE Transactions on 25(9)

[99] N. I. Cho and S. U. Lee, Fast algorithm and implementation of 2-D discrete cosine transform. Circuits and Systems (1991), IEEE Transactions on, 38(3), 297-305.

[100] F. A. Kamangar and K. R. Rao, Fast algorithms for the 2-D discrete cosine transform. Computers (1982), IEEE Transactions on, 100(9), 899-906.

[101] V. K. SHARMA, K . MAHAPATRA and U. C. PATI, non-recursive computation of 8×8 2D DCT for high accuracy and low area. Journal of Circuits, Systems, and Computers, 23(10), (2014).

[102] E. Feig and E. Linzer. The multiplicative complexity of discrete cosine transforms. Advances in Applied Mathematics, 13(4), (1992), 494-503.

[103] S Bouguezel, MO Ahmad, MNS Swamy, A multiplication-free transform for image compression, in The 2nd Int. Conf. Signals, Circuits and Systems, 2008, pp. 1–4

[104] S Bouguezel, MO Ahmad, MNS Swamy, A fast 8x8 transform for image compression, in Proceeding of the 2009 Int. Conf. on Microelectronics (ICM) (Marrakech, 2009), pp. 74–77. doi: 10.1109/ICM.2009.5418584

[105] S Bouguezel, MO Ahmad, MNS Swamy, A novel transform for image compression, in The 53rd IEEE Int. Midwest Symp. Circuits and Systems (MWSCAS), 2010, pp. 509 512

[106] S Bouguezel, MO Ahmad, MNS Swamy, A low-complexity parametric transform for image compression, in Proceeding of the 2011 IEEE Int. Symp. Circuits and Systems (Rio de Janeiro, 2011), pp. 2145–2148

[107] Dhandapani, Vaithiyanathan, and Seshasayanan Ramachandran. "Area and power efficient DCT architecture for image compression." EURASIP Journal on Advances in Signal Processing 2014, no. 1 (2014): 1-9.

[108] Vaithiyanathan, D., et al. "A low-complexity DCT approximation for image compression with 14 additions only." *Green Computing, Communication and Conservation of Energy (ICGCE), 2013 International Conference on*. IEEE, 2013.

[109] Wang, Z., & Bovik, A. C." Reduced-and no-reference image quality assessment". Signal Processing Magazine, IEEE, 28(6), 29-40.(2011)

[110] M. Jridi, A. Alfalou, and P.K. Meher, "a generalized algorithm and reconfigurable architecture for efficient and scalable orthogonal approximation of dct," IEEE Trans. Circuits Syst. 62(2), 449 - 457, (2014).

[111] Cucchiara, Rita, et al. "Using a wireless sensor network to enhance video surveillance." journal of ubiquitous computing and intelligence 1.2 -187-196 (2007).

[112] Ye, Yun, et al. "Wireless video surveillance: A survey." *IEEE Access* 1 (2013): 646-660.

[113] Radke, Richard J., et al. "Image change detection algorithms: a systematic survey." *IEEE transactions on image processing* 14.3 (2005): 294-307.

[114] Rodrigues, Marco Túlio AN, et al. "Change detection based on features invariant to monotonic transforms and spatially constrained matching." *Journal of Electronic Imaging* 25.1 (2016): 013001-013001.

[115] Seetharaman, Gunasekaran, et al. "System and method for static and moving object detection." U.S. Patent No. 9,454,819. 27 Sep. 2016.

[116] Martínez-de Dios, J. R., A. Jiménez-González, and A. Ollero. *Localization and Tracking Using Camera-Based Wireless Sensor Networks*. INTECH Open Access Publisher, 2011.

[117] Alhilal, Mohsin S., Adel Soudani, and Abdullah Al-Dhelaan. "Low power scheme for image based object identification in wireless multimedia sensor networks." *Multimedia Computing and Systems (ICMCS), 2014 International Conference on*. IEEE, 2014.

[118] P. Rosin, "Thresholding for change detection," *Comput. Vis. Image Understanding*, vol. 86, no. 2, pp. 79–95, May 2002.

[119] P. Rosin and E. Ioannidis, "Evaluation of global image thresholding for change detection," *Pattern Recognit. Lett.*, vol. 24, no. 14, pp. 2345–2356, Oct. 2003.

[120] P. Smits and A. Annoni, "Toward specification-driven change detection," *IEEE Trans. Geosci. Remote Sens.*, vol. 38, no. 3, pp. 1484–1488, May 2000.

[121] PETS2000 Dataset: http://www.cvg.reading.ac.uk/datasets/ accessed 2017

[122] pedastrians Datasets http://wordpress-jodoin.dmi.usherb.ca/dataset2014/ accessed 2017

[123] SIPI Database: http://sipi.usc.edu/database/ accessed 2017

[124] Karakus, Celalettin, Ali Cafer Gurbuz, and Bulent Tavli. "Analysis of energy efficiency of compressive sensing in wireless sensor networks." *IEEE Sensors Journal* 13.5 (2013): 1999-2008.